



UNIVERSITY OF LEEDS

This is a repository copy of *Influence of fluvial crevasse-splay deposits on sandbody connectivity: Lessons from geological analogues and stochastic modelling*.

White Rose Research Online URL for this paper:
<https://eprints.whiterose.ac.uk/172518/>

Version: Accepted Version

Article:

Colombera, L orcid.org/0000-0001-9116-1800 and Mountney, NP orcid.org/0000-0002-8356-9889 (2021) Influence of fluvial crevasse-splay deposits on sandbody connectivity: Lessons from geological analogues and stochastic modelling. *Marine and Petroleum Geology*, 128. 105060. ISSN 0264-8172

<https://doi.org/10.1016/j.marpetgeo.2021.105060>

© 2021, Elsevier. This manuscript version is made available under the CC-BY-NC-ND 4.0 license <http://creativecommons.org/licenses/by-nc-nd/4.0/>.

Reuse

This article is distributed under the terms of the Creative Commons Attribution-NonCommercial-NoDerivs (CC BY-NC-ND) licence. This licence only allows you to download this work and share it with others as long as you credit the authors, but you can't change the article in any way or use it commercially. More information and the full terms of the licence here: <https://creativecommons.org/licenses/>

Takedown

If you consider content in White Rose Research Online to be in breach of UK law, please notify us by emailing eprints@whiterose.ac.uk including the URL of the record and the reason for the withdrawal request.



eprints@whiterose.ac.uk
<https://eprints.whiterose.ac.uk/>

Influence of fluvial crevasse-splay deposits on sandbody connectivity: lessons from geological analogues and stochastic modelling

Luca Colombera*, Nigel P. Mountney

Fluvial, Eolian & Shallow-Marine Research Group, School of Earth & Environment, University of Leeds, LS2 9JT, Leeds, UK

*) corresponding author: l.colombera@leeds.ac.uk

Abstract

To investigate the importance of crevasse-splay elements for the connectivity of fluvial sandbodies, an integrated study has been undertaken that combines data from outcropping and subsurface fluvial successions, and modern rivers, with outputs from forward stratigraphic models and object-based modelling. Literature-derived analogue data on over 2,100 crevasse-splay elements from many fluvial systems have been synthesized to obtain quantifications of the proportion and geometry of crevasse-splay units, and of their topological relationships with channel deposits. Some of the analogue data are used to inform inputs to stochastic modelling that is applied to determine how the presence of crevasse-splay deposits affects the connectivity of successions in which channel sandstones are preserved as channelized bodies or compartmentalized point-bar units. Architectural configurations are documented that are variably characterized by (i) crevasse-splay sandbody compartmentalization, (ii) channel-sandbody connections that increase sandbody size and the likelihood of borehole connectivity, and (iii) intercommunication between different channel sandbodies. Analyses of analogue data demonstrate scaling relationships between the morphometry of crevasse-splay elements and associated channel elements and river catchments. Results also demonstrate how the proportions of channel and crevasse-splay deposits tend to covary in stratigraphic volumes. This information, when ported to stochastic models, yields results showing how the influence of crevasse-splay elements on static connectivity varies – in relative terms – as a function of architectural style, net-to-gross ratio and channel-sandbody geometry. Channel-body connections may be more important for smaller and relatively sand-poor fluvial systems, whereas mud-plug compartmentalization of splay elements may be more important for successions with larger channel-body width-to-thickness aspect ratios and lower net-to-gross ratios. The results of this work can be applied to facilitate and improve the characterization and modelling of the static connectivity of subsurface successions that include crevasse-splay deposits. The results also reveal the possible influence of certain geological controls (channel avulsion, river-system scale, overbank cannibalization) on static connectivity.

Keywords: overbank; fluvial reservoir; static connectivity; stratigraphic compartmentalization; sedimentary architecture; fluvial architecture; reservoir modeling; subsurface characterization.

1. Introduction

Crevasse splays are conspicuous features of fluvial landscapes and of the sedimentary record of floodbasins. In subsurface fluvial successions, crevasse-splay deposits typically form relatively porous and permeable sandbodies, which can act as productive units in hydrocarbon reservoirs (e.g., Jirik 1990; Chapin & Mayer 1991, Ramón & Cross 1997; Stuart et al., 2014; Heldreich et al. 2017; Ba et al. 2019), and as significant components of alluvial aquifers (e.g., Bersezio et al. 2004; Grasby et al. 2008; Maliva 2016; Dall’Alba et al. 2020).

Despite their common and widely recognized contribution to permeable volumes, the role of crevasse-splay units on static connectivity can be difficult to predict. It is commonly assumed that the presence of crevasse-splay deposits will increase the lateral connectivity of sandbodies, via their role in acting as

conduits that link larger fluvial channel bodies (Mjøs et al. 1993; Hornung & Aigner 1999; Larue & Hovadik 2006; Bos & Stouthamer 2011; Miall 2014; van Tooreneburg et al. 2016; Burns et al. 2017; Yeste et al. 2020), and that overall this will increase reservoir performance (Miall 2014). However, it is also recognized that, because of their geometry and position relative to channel sandbodies, crevasse-splay deposits may form isolated stratigraphic compartments or poorly connected units, which need to be penetrated by wells to enable production of the hydrocarbons they may contain (e.g., Ambrose & Jackson 1989; Ambrose et al. 1991; Tyler & Finley 1991).

The importance of crevasse-splay deposits in controlling the static and dynamic connectivity of fluvial successions has already been the subject of field-based and numerical-modelling studies (e.g., McKenna & Smith 2004; Jones & Hajek 2007; Burns et al. 2010a,b; Pranter & Sommer 2011; Sloan 2012). Notwithstanding, some important aspects of the ways in which the occurrence and characteristics of crevasse-splay deposits control the connectivity of fluvial sandbodies still need to be elucidated. In particular, it is of practical importance to determine how the influence of crevasse-splay sandbodies on static connectivity varies in relation to characteristics of the sedimentary architecture of fluvial successions, notably the proportions of deposits of different origin, or the topology of architectural elements, for example. This work addresses this problem through the characterization of a range of modern and ancient geological analogues, and through the use of process-based and object-based stochastic modelling techniques.

The aim of this work is to facilitate and improve the characterization and modelling of the static connectivity of subsurface successions of fluvial origin that include crevasse-splay deposits. This is achieved through the following interrelated objectives: (i) the synthesis and quantitative documentation of a range of architectural styles seen in nature; (ii) the definition of constraints of geological realism for models of subsurface successions that incorporate splay elements; and – partly using these constraints – (iii) the determination of the role of crevasse splays in controlling the static connectivity of fluvial sandbodies.

2. Background

Crevasse splays are flood-fed lobe-shaped sediment accumulations deposited at the outlet of levee breaches in fluvial floodbasins (Bridge 2006). Their genesis is related to the incision of crevasses in the banks and levees of channels, which typically occurs close to the time of peak-flood conditions. This is followed by the emplacement of splay deposits across a floodbasin during the falling stage, and in some cases in relation to successive floods (Zwoliński 1992; Yuill et al. 2016). A crevasse splay can be fed by sediment derived from the remobilization of levee material, particularly at the time the levee is breached (e.g., Ortega & Garzón Heydt 2009), but can then grow through supply of suspended sediment fed by the parent river channel, which may occur during multiple floods over the entire lifetime of the splay (Millard et al. 2017). The term ‘crevasse splay’ is commonly used to refer to geomorphic features and deposits of river floodplains, where their inception may be heralding the avulsion of trunk river channels (Smith et al. 1989; Slingerland & Smith 2004; Hajek & Edmonds 2014; Słowik 2018). However, in this work, and as is common to other studies, the term is also applied to lacustrine deltas that are fed through levee breaks and build out in static water bodies bordering channel belts (cf. Miall 1996). Other sedimentary units that are similar in characteristics or genesis include: (i) overbank sands formed by levee overtopping during floods (cf. Kurowski 1999; van de Lageweg et al. 2013; Lewin et al. 2017) and which are sometimes present as the pre-breach substrate of crevasse splays (e.g., Sato et al. 2017); (ii) crevasse sub deltas that grow in marginal-marine interdistributary bays, which are also commonly termed ‘crevasse splays’ (Arndorfer 1973; Elliott 1974; Wright 1985). These overbank splays and crevasse subdeltas are not explicitly considered in this paper, but some of the data from the ancient rock record that is presented herein may still relate to units that are comparable in origin to these types, given the uncertainty in discriminating these features in the stratigraphic record.

The geomorphology and internal anatomy of crevasse splays, and the associated drainage of crevasse channels, can exhibit significant diversity in nature (Fig. 1). Typically, crevasse splays are fan-like or lobate units (Bridge 2006), and these geometries are usually assumed when crevasse-splay deposits are incorporated in geocellular models of subsurface successions (Deutsch & Tran 2002; Keogh et al. 2007; Donoso 2016; Vevle et al. 2018; Li et al. 2019). In reality, however, crevasse splays can take irregular

forms, and commonly display digitate shapes in planform (cf. O'Brien & Wells 1986; Gębica & Sokołowski 2001; Makaske 2001; Arnaud-Fassetta 2013; Toonen et al. 2016; Nichols & Viers 2017). The observed variability in the anatomy of crevasse splays reflects in part their different modes and histories of accretion. For example, crevasse splays can develop as simple lobes at the terminus of a crevasse (Fig. 1D), can be built by the propagation of intricate distributary networks of crevasse channels (Fig. 1A,F,G), or can be constructed as a set of diachronous coalescing lobes by local avulsions along the main crevasse feeder (Fig. 1H). These different forms might also correspond to different stages of the evolutionary development of splays, from inception to maturity (Smith et al. 1989).

Crevasse splays are highly variable in scale, ranging from tens of metres to kilometres in diameter (Mjøs et al. 1993; Reynolds 1999; Millard et al. 2017). They may also be highly variable in lithology. Crevasse splays tend to form as sand-rich accumulations, since sand transported in suspension by the river channel and through levee breaches will tend to be deposited in channel-proximal positions due to flow expansion (Millard et al. 2017). It has long been recognized, however, that the view of splays as sandy lenses is simplistic (Smith & Pérez-Arlucea 1994). Commonly, only the proximal part of crevasse-splay deposits may be sandy (Bos & Stouthamer 2011; Arnaud-Fassetta 2013; Toonen et al. 2016; Burns et al. 2017; Gulliford et al. 2017; Yeste et al. 2020); in some cases, crevasse splays are dominantly muddy (e.g., Gharibreza et al. 2014) or even almost entirely made of clay and silt (e.g., Staub & Cohen 1979). Some crevasse splays may be characterized by proximal-to-distal grain size fining, and by coarsening-upward trends reflecting crevasse-splay progradation on the floodplain (Jones & Hajek 2007; Burns et al. 2017; Gulliford et al. 2017; Yeste et al. 2020). In these cases, the most porous volume may be restricted to the most proximal and upper part of a crevasse-splay unit. However, more complex facies distributions may also exist in three dimensions, for example if sand accumulation is limited to crevasse-channel mouths (e.g., Guion 1984; Farrell 2001; Turner & Tester 2006).

A striking characteristic of river systems is the variability in the frequency of occurrence of crevasse splays along river courses. Some river reaches are apparently devoid of them, whereas others are characterized by channel belts bordered by numerous splays (e.g., Syvitski et al. 2012; van Toonenburg et al. 2018; Nienhuis 2019; Iacobucci et al. 2020). In some circumstances, crevasse splays may be seen frequently along a river channel, but their preservation potential may be limited, for example where they are associated with a river that is constrained to wander within the confines of a valley, or because of preferential crevasse-splay occurrence on outer banks undergoing erosion in mobile meandering rivers (Kesel 1988).

Together with their abundance, size and lithology, a number of architectural characteristics of crevasse-splay deposits are likely to determine their role in controlling sandbody connectivity. When constructing models of the architecture of subsurface fluvial successions, it is relatively common to view crevasse-splay deposits as fully connected to channel bodies, themselves treated as tanks of sand (e.g., Fig. 2A). However, splay deposits may be fully disconnected from channel-belt deposits or have limited connectivity. Primary sandbody connectivity, arising as an inherent property of depositional architectures, may only exist where crevasse splays are physically linked to sand-prone infills of the channels from which they originated or to sandy barform elements preserving their banks (e.g., Mjøs et al. 1993). Crevasse splays may not be originally connected to channel sandbodies where they emanate from abandoned channel forms infilled by mud plugs (e.g., Fig. 1B, 2C), or where they border mud-rich eddy-accretion packages (e.g., Fig. 1C). Furthermore, levee failure and flow constriction through crevasses may cause extensive scour in proximity of a channel (Gomez et al. 1995, 1997; Jacobson & Oberg 1997; Gębica & Sokołowski 2002; Matsumoto et al. 2016), resulting in elongated scour pits and areas of widespread shallow erosion termed 'stripped zones' (Gomez et al. 1997; Fig. 2D): in such cases physical connectivity between crevasse-splay and channel sands will depend on the nature of the infill of these erosional forms. Crevasse splays may also form isolated sandbodies if levee breaches are filled with mud (e.g., Galloway 1977), whereas in finer-grained splays, conversely, sand deposition may be largely restricted to crevasse-channel fills (e.g., Stuart et al. 2014). Detachment from channel-belt deposits can also occur if crevasse-splay sand accumulation takes the form of mouth bars at the termini of crevasse channels, as may happen in lacustrine deltas (e.g., Farrell 2001) (Fig. 2E). These are all situations that can give rise to stratigraphic compartmentalization of fluvial successions. However, secondary connectivity between genetically unrelated channel sandbodies and crevasse-splay deposits

may still arise from overbank cannibalization by laterally mobile river channels (e.g., Donselaar & Overeem 2008).

Other factors can influence whether crevasse-splay sands act as connectors between different channel sandbodies. Where crevasse splays are fully contained within the boundaries of channel belts (e.g., Garzón & Alonso 2002; Joeckel et al. 2016; Fig. 1I), they can potentially create communications between stratigraphic compartments that exist internally in the channel bodies (cf. Donselaar & Overeem 2008; Colombera et al. 2017), but they will have no effect on sand connectivity across different channel belts. Primary connections may be established between channel belts that co-existed as active and/or abandoned features on the floodplain (Fig. 2B). Nevertheless, the development of these connections is unlikely where channel belts fully occupy the floor of an incised valleys (cf. Syvitski et al. 2012), since channel spillage would be constrained by the interfluves. Primary connectivity across channel sandbodies may instead require amalgamation of splays emanating from different channel belts that themselves form elevated alluvial ridges, since splays will be restricted to depressions between accretionary belts (Lewin et al. 2017). Secondary linkages between different channel bodies, occurring because of the lateral or vertical erosion of overbank by other channel belts, are likely to be more important: thanks to these, vertical and lateral sandbody connectivity can both be enhanced, to a degree that will depend on the spatial relationships of the sedimentary units (Fig. 2B).

Sandbody connectivity may also arise depending on the style of interaction of different crevasse-splay elements. For example, the lateral coalescence of crevasse splays neighbouring a levee may result in sandbody amalgamation (van Tooreneburg et al. 2016, 2018; Burns et al. 2017, 2019; Fig. 1A,F,G). Where sand deposition is mostly restricted to crevasse-channel fills, instead, sandbody communication may result from the intersection of different crevasse-channel networks (e.g., Makaske et al. 2017; Fig. 1E), albeit possibly in the form of a so-called labyrinthine architecture (*sensu* Webber & van Geuns 1990), which can display high sandbody tortuosity.

Within crevasse-splay deposits, sand-body compartmentalization may exist where they are internally organized into depositional lobes, due to avulsive lobe switching or distributary drainage (cf. Fielding 1984a,b, 1986; Smith et al. 1989; Toonen et al. 2016; Sato et al. 2017). In these situations, a hierarchy of sandy lobes can develop inside splays (Florsheim & Mount 2002; Arnaud-Fassetta 2013; Burns et al. 2017, 2019), which may be stacked compensationally (e.g., Guion et al. 1995) and may be partitioned by distal-splay, lacustrine or overbank fines. Crevasse sands can also be deposited in disconnected pockets where they heal irregular floodplain topography (cf. van Dinter & van Zijverden 2010; Bigi et al. 2015). Additionally, internal compartmentalization may be caused by mud plugs that represent the fine-grained infill of crevasse-channel networks (e.g., Smith & Pérez-Arlucea 1994).

Several factors control the size, lithology, proportion and spatial distribution of crevasse-splay deposits, and hence their role in determining sandbody connectivity in fluvial successions. A comprehensive summary of these controls is beyond the scope of this work; nonetheless, it must be acknowledged that recognition of the influence of controlling factors in the stratigraphic record has value for predicting architectural styles and guiding subsurface geological modelling.

For instance, tectonics, base-level and hinterland controls on river equilibrium profile drive accommodation generation, which in turn exerts influence on the preservation and topology of overbank deposits, where these are reworked by migrating and avulsing channels (Allen 1978; Bridge and Leeder 1979). The rate of creation of accommodation additionally controls the likelihood of levee crevassing and crevasse-splay characteristics, by determining the rate at which alluvial ridges and associated levees are constructed to attain superelevation over the neighbouring floodplain. Channel superelevation itself dictates the establishment of cross-floodplain water-surface and levee gradients that favour crevasse-splay formation (Slingerland & Smith 1998; Mohrig et al. 2000; Millard et al. 2017). The role of accommodation as a driver of channel vertical accretion and avulsion is reflected in the preserved sedimentary records of some anastomosing river systems, which tend to be highly avulsive and are prone to contain abundant crevasse-splay deposits (Makaske 2001; Makaske et al. 2002; Bernal et al. 2013). By contrast, longer channel-belt interavulsion periods determine longer times over which levees can aggrade and crevasse splays can develop and grow, and this may be reflected in the abundance and size of crevasse-splay elements in overbank stratigraphies.

Crevasse-splay sedimentation is also governed by the climate of river floodplains and catchments, chiefly through its controls on water and sediment delivery, floodplain drainage state, water-discharge regime and floodplain vegetation. For example, the rate of sediment supply can determine the abundance of crevasse-splay deposits by regulating the rate of channel aggradation and by controlling the nature of overbank sedimentation, which by affecting sediment-compaction rate and land subsidence determines the longevity of crevasses (Makaske et al. 2017; Nienhuis et al. 2018). The drainage conditions of a floodplain also influence the likelihood and extent of crevasse-splay deposition, by dictating the water-surface slope away from the river channel (Aalto et al. 2003; Adams et al. 2004; Millard et al. 2017), and by causing flow deceleration where the water table is exposed to allow development of static water bodies such as floodplain ponds and lakes (Bristow et al. 1999); these controls are expected to be reflected in contrasting sedimentary records of arid and humid floodplains (Yeste et al. 2020). Furthermore, dryland rivers tend to exhibit a downstream decrease in channel hydraulic geometry, partly due to transmission losses, which can make the lower reaches of these rivers particularly susceptible to overbank deposition (Donselaar et al. 2013; van Toorenenburg et al. 2016). A climatic control is also mediated by vegetation, which, acting as stabilizing agent, can affect levee erodibility and the morphology and drainage pattern of crevasse splays (Nienhuis et al. 2018).

In addition to climate, catchment controls are determined by the physiography and size of drainage areas and associated river systems. These factors affect the concentration of suspended sediment of flood events that feed crevasse splays (Kesel 1988). For a given river system, sediment concentration during floods and total suspended-sediment load both tend to be scaled to water discharge (Williams 1989, Milliman & Farnsworth 2011). The characteristics of crevasse splays may also be affected by the water-discharge regime; compared to perennial rivers, ephemeral fluvial systems experiencing flash floods tend to be characterized by events with a significantly higher concentration of sediment (Reid & Frostick 2011), which can nourish crevasse splays, as well as by rapid flood recessions, which may limit the development of crevasse-channel networks (Bristow et al. 1999). The calibre of the material transported through a river system will instead control the fraction of sediment that, during a flood, can be transferred in suspension to the overbank, and the degree to which proximal-to-distal grain size trends develop along the profile of a splay (Millard et al. 2017).

A set of downstream controls on crevasse-splay formation and characteristics may also operate in lower fluvial reaches, due to the influence of marine processes on river morphodynamics. This includes for example the role of backwater effects in modulating river flow (Lamb et al. 2012; Nittrouer et al. 2012), whose importance on overbank sedimentation is not well known. It has been suggested that drawdown of the channel water surface occurring in the backwater zone during high flow stage (Lamb et al. 2012), by attenuating cross-floodplain water-surface gradients, could inhibit crevasse-splay deposition (Colombera et al. 2016). This may in part explain trends of downstream decrease in the size of crevasse splays (cf. Nienhuis 2019) and in the proportion of their deposits (cf. Bos & Stouthamer 2011).

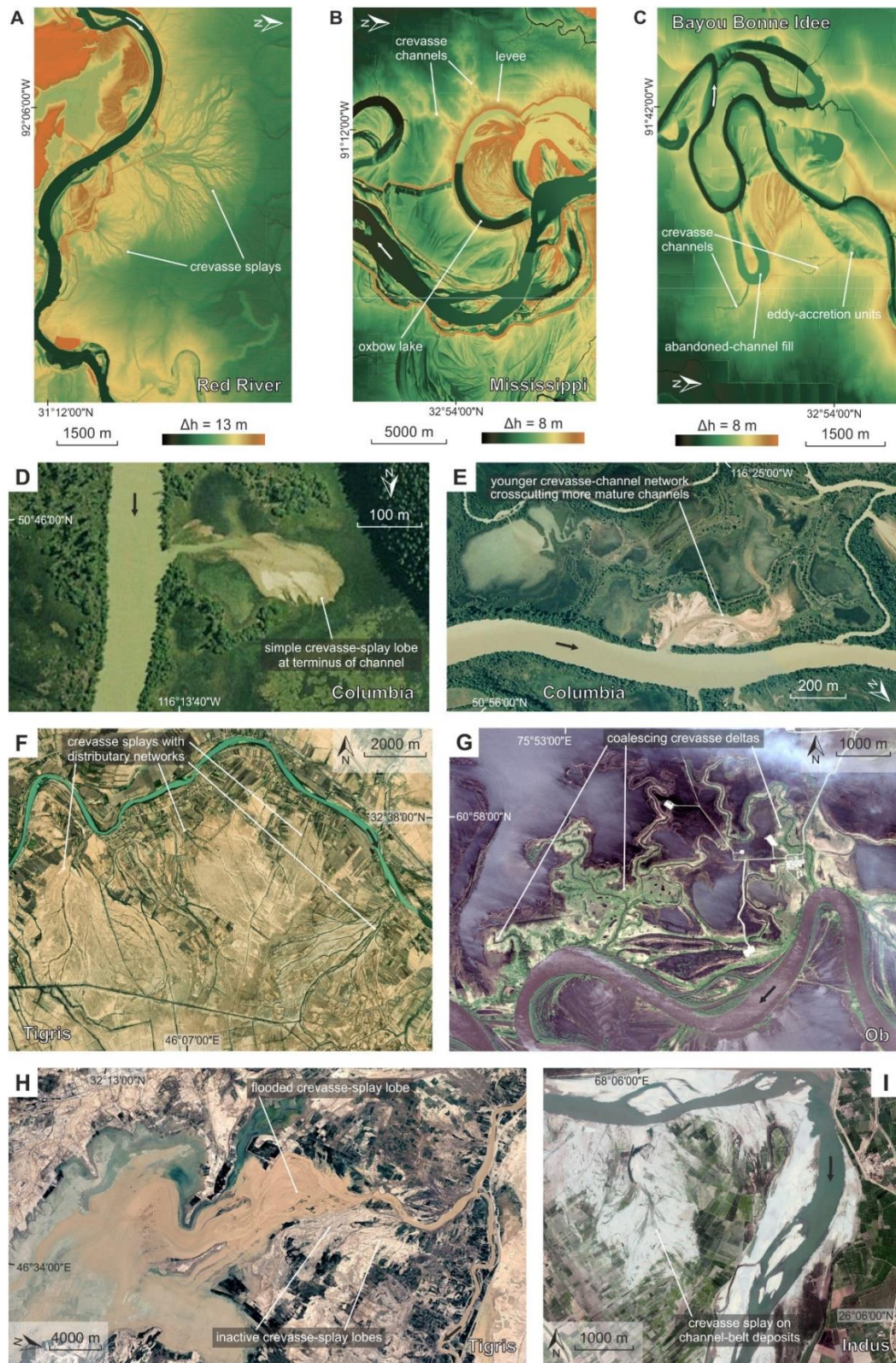


Figure 1: Forms of modern crevasse splays. (A) LiDAR topography of coalescing crevasse splays of the Red River, Louisiana, USA. (B) LiDAR topography of overbank landforms of the Mississippi, Louisiana-Mississippi, USA. (C) LiDAR topography of overbank landforms of the Bayou Bonne Idee, Louisiana, USA. (D-E) Satellite images of crevasse splays of the Columbia River, British Columbia, Canada. (F) Satellite image of crevasse splays of the Tigris, Iraq. (G) Satellite image of crevasse splays of the Ob, Russia. (H) Satellite image of a partially flooded crevasse splay of the Tigris, Iraq, December 1988. (I) Satellite image of a crevasse splay of the Indus, Pakistan. LiDAR data from USGS; satellite imagery from GoogleEarth.

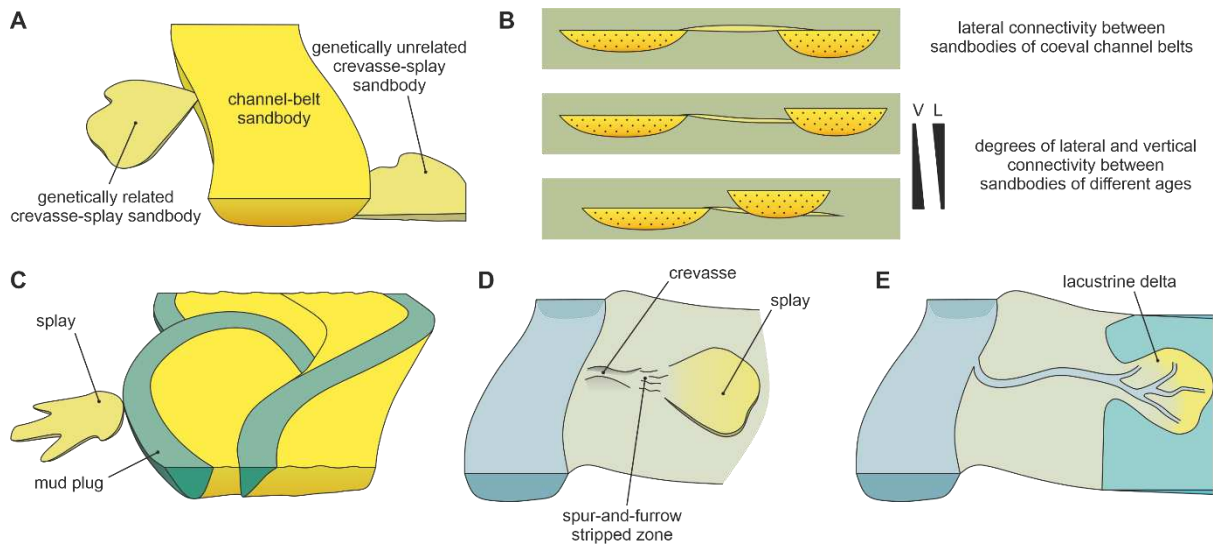


Figure 2: Types and degrees of connectivity between channel and crevasse-splay units. (A) Physically connected channel and crevasse-splay sandbodies; primary sandbody connectivity exists with splay deposits that are genetically related with the channel-belt sandbody, whereas secondary connectivity between these channel deposits and splay elements that are genetically related to different channel belts are established by channel-bank erosion. (B) Lateral and vertical static connectivity between different channel bodies mediated by crevasse-splay units. (C) Crevasse-splay sands compartmentalized by a mud-prone abandoned-channel fill. (D) Crevasse-splay sands that are not physically connected with their parent channel form due to erosional floodplain features. (E) Crevasse-splay sands that accumulate as lacustrine-delta mouth bars distally away from a trunk river channel.

3. Data and methods

This work integrates results of analyses undertaken on the following data types and modelling outputs (Fig. 3): (i) literature-derived data of crevasse-splay elements recognized on modern river floodplains and in the ancient and Quaternary stratigraphic record, stored in a sedimentological database (FAKTS; Colombera et al. 2012a,b, 2013); (ii) outputs of a stochastic process-based forward model that simulates the accumulation of fluvial successions of meandering river systems (FLUMY; Cojan et al. 2004; Grappe 2014); (iii) geocellular models produced using an object-based stochastic modelling algorithm (TETRIS; Boucher et al. 2010). Details on each component of this work are provided next.

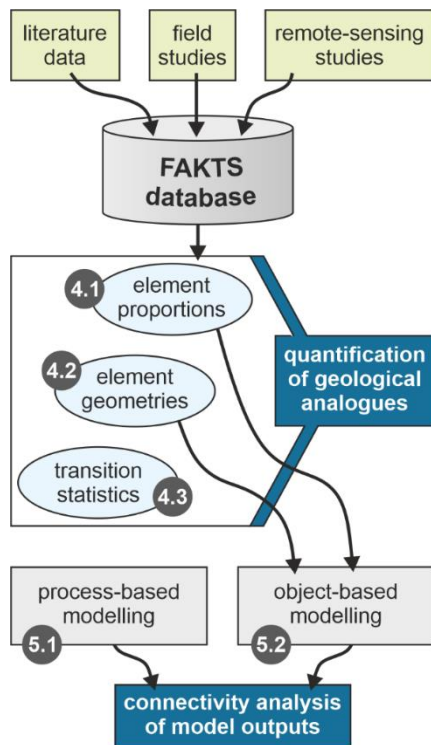


Figure 3: Flow chart summarizing the components of the work, types of data sources, and how database and modelling outputs are employed in the analyses. The circled numbers indicate the sections of the article where the labelled subjects are specifically presented.

3.1. FAKTS: database and limitations

Data on the form and sedimentology of modern and ancient crevasse-splay elements were collated from many published sources and stored in a SQL relational database, the Fluvial Architecture Knowledge Transfer System (FAKTS; Colombera et al. 2012b). In FAKTS, the sedimentary architecture of fluvial successions and geomorphic organization of river systems are digitized in the form of hard and soft data assigned to a hierarchy of genetic units, ranging from large-scale ‘depositional elements’ to sub-bed-scale ‘facies units’ (Colombera et al. 2012a,b, 2013). FAKTS records the geometry, spatial relationships, and hierarchical relationships of these different types of sedimentary units. These units are assigned to ‘subsets’ of fluvial systems, which can represent, for example, different reaches of the same river, or different intervals of a stratigraphic succession. Subsets are classified on parameters that describe the depositional systems and their controlling factors.

Individual crevasse splays are documented in FAKTS as intermediate-scale units termed ‘architectural elements’, which can be part of floodplain depositional elements, and for which several attributes (e.g., morphometric parameters) and spatial transitions to other architectural elements are recorded. FAKTS can therefore be queried to generate outputs on the occurrence, size and transition statistics of crevasse-splay elements and associated sedimentary units in classified fluvial systems.

The data analysed in this study relate to a total of over 2,100 crevasse-splay elements, associated with 36 modern rivers and over 40 fluvial successions, and have been derived from 84 literature sources consisting of scientific papers or dissertations (Table 1), complemented with unpublished field data (Colombera et al. 2012a) and interpretations of satellite imagery (Shiers 2016).

The database analysis presented in this paper is subject to some limitations. To allow for the integration of data from disparate datasets, the data are standardized – to some degree – as part of the process of database collation; yet, facts and interpretations by the original authors are relied upon, and discrepancies may exist across the datasets that are included. Ancient examples of crevasse-splay deposits are interpreted from the stratigraphic record, where distinction from other types of overbank sandbodies is uncertain. Dimensional data relating to examples from outcrop studies are affected by the quality, three-dimensionality, orientation and extent of outcrop exposure. Any comparison of modern landforms with preserved sedimentary bodies will not account for preservation potential. Moreover, the finite evolution of modern forms is not captured in splays that are still active. Comparisons of the size

of crevasse-splay elements is affected by variability in criteria chosen for placing their distal boundaries (e.g., lithological, geometric): these may vary depending on approaches taken by different authors, and particularly between ancient and modern units. Also, the inclusion of data from river systems subject to anthropogenic activity has some implications. Examples are included in which artificial levees exist, which may sustain higher hydraulic head than natural levees, causing comparatively more energetic levee failures; the material forming artificial levees, which is ultimately remobilized into splays, may also differ from that of natural levees in terms of available volume and grain size (Jacobson & Oberg 1997; Gębica & Sokołowski 2001). It is significant in this respect that the database includes examples of intentional artificial-levee breaks (cf. Florsheim & Mount 2003). The presence of dams along river courses modulates water discharge and the concentration and grain size of suspended sediment (e.g., Yu et al. 2014); these controls are likely to affect the development and characteristics of crevasse splays. Agriculture is also an important factor when considering modern floodplains as analogues to the rock record: agricultural activity affects the erodibility and roughness of floodplains (Jacobson & Oberg 1997), and may involve the removal of crevasse-splay sands where these form sterile soils (Azevêdo et al. 2004) or the modification of natural crevasse-channel networks for irrigation purposes (Wilkinson et al. 2015).

Table 1: Summary of FAKTS case studies of ancient successions and modern rivers considered in this work; references to primary data sources are reported.

Analogue type	Case study	References
Ancient	Middle-Upper Stubensandstein	Hornung & Aigner (1999)
	Quaternary Po Basin	Amorosi et al. (2008)
	Lower Williams Fork Fm.	Pranter et al. (2009)
	Upper Unit, Tortola fluvial system	Cuevas Gozalo & Martinius (1993)
	Organ Rock Fm.	Cain (2009; see Cain & Mountney 2009)
	Kayenta Fm.	Original study (see Colombera et al. 2012a)
	Quaternary Rhine-Meuse delta	Weerts & Bierkens (1993)
	Sariñena Fm.	Donselaar & Overeem (2008)
	Olson Mb., Escanilla Fm.	Labourdette (2011)
	Omingonde Fm.	Holzförster et al. (1999)
	Dinosaur Canyon Mb., Moenave Fm.	Olsen (1989)
	Balfour Fm., Beaufort Gp.	Catuneanu & Elango (2001)
	Middleton Fm. and Koonap Fm., Beaufort Gp.	Catuneanu & Bowker (2001)
	Fairlight Clay and Ashdown Beds Fm., Hastings Beds Gp.	Stewart (1983)
	Joggins Fm.	Rygel & Gibling (2006)
	Templetown Fm. (Brownstown Head Mb. and Beenlea Head Mb.) and Harrylock Fm., Old Red Sandstone	Ori & Penney (1982)
	Buntsandstein	Sánchez-Moya et al. (1996)
	Vinchina Fm.	Limarino et al. (2001)
	Warchha Sandstone Fm., Nilawahān Gp.	Ghazi & Mountney (2009)
	Abo Fm.	Mack et al. (2003)
Kaiparowits Fm.	Roberts (2007)	
Willwood Fm.	Kraus & Middleton (1987)	
Chinle Fm.	Trendell et al. (2013)	

	Colton Fm.	Rasmussen (2005)
	Middle Wasatch Fm.	Ford & Pyles (2014)
	Lower Wasatch Fm.	Sendziak (2012)
	Upper Chickaloon Fm.	Flores & Stricker (1993)
	Scalby Fm.	Ielpi & Ghinassi (2014)
	Iles Fm., Mesaverde Gp.	Anderson (2005); Jones et al (1987)
	Teekloof Fm., Beaufort Gp.	Smith (1987)
	Neslen Fm., Mesaverde Gp.	Original study (see Burns et al. 2017)
	Castlegate Fm., Mesaverde Gp.	Original study (see Burns et al. 2017)
	Salt Wash Mb., Morrison Fm.	Original study (see Burns et al. 2017)
	Callide Seam Mb., Callide Coal Measures	Jorgensen & Fielding (1996)
	Ravenscar Gp.	Mjøs et al. (1993)
	Abrahamskraal Fm., Beaufort G	Gulliford et al. (2017)
	Grey Clays Mb., Poznan Fm.	Widera (2016); Chomiak (2020)
	Grey Clays Mb., Poznan Fm.	Chomiak et al. (2019)
	Tabular cover of the Iberian Meseta (TIBEM)	Yeste et al. (2020)
	Elliot Fm., Stormberg Gp.	Visser & Botha (1980)
	Lunde Fm.	Nordahl et al. (2014)
	Blackhawk Fm.	Sahoo et al. (2016)
Modern	Amargosa	Ielpi (2019)
	Ashepoo	Staub & Cohen (1979)
	Bayou Lafourche (Mississippi)	Esposito et al. (2017); Shen et al. (2015)
	Bayou Lafourche (Mississippi)	Nienhuis (2019)
	Cosumnes	Nichols & Viers (2017)
	Cosumnes	Florsheim & Mount (2002)
	Euphrates	Wilkinson et al. (2015); Jotheri et al. (2018); Jotheri & Allen (2020)
	Guadarrama	Garzón & Alonso (1996, 2002)
	Jarama	Garzón & Alonso (2002)
	Jarrahi	Walstra et al. (2010)
	Rivers of Helodrano Mahajambe	Burns et al. (2019)
	Palaeo-Karun-Karkheh	Heyvaert et al. (2012, 2013); Heyvaert & Walstra (2016)
	Kinu	Matsumoto et al. (2016)
	Little Blue River	Joeckel et al. (2016)
	Mahajamba	Original study
	Mahajamba	Burns et al. (2019)
	Mississippi	Jordan & Pryor (1992)
	Mississippi	Burns et al. (2019)
	Mississippi	Farrell (1987)
	Mississippi	Gomez et al. (1997)
	Mississippi	Jacobson & Oberg (1997)
	Mossy River (Saskatchewan)	Smith & Pérez-Arlucea (1994)
	Niobrara	Burns et al. (2019)
	Niobrara	Bristow et al. (1999)

	Paraná	Burns et al. (2019)
	Pastaza	Bernal et al. (2013)
	Rhine	Burns et al. (2019)
	Rhône	Arnaud-Fassetta (2013)
	Río Colorado/Río Capilla	Donselaar et al. (2013); Li et al. (2015); Perdomo Figueroa (2017)
	Saloum	Burns et al. (2019)
	Sandover	Millard et al. (2017)
	Sandy Creek (Timbarra River tributary)	O'Brien & Wells (1986)
	Saskatchewan	Millard et al. (2017)
	Saskatchewan	Burns et al. (2019)
	Saskatchewan	Toonen et al. (2016)
	Saskatchewan	Farrell (2001)
	Saskatchewan	Pérez-Arlucea & Smith (1999)
	Secchia	Bigi et al. (2015)
	Sofia	Burns et al. (2019)
	Tigris	Morozova (2005)
	Tigris	Jotheri (2018)
	Tigris	Jotheri et al. (2018)
	Tuross	Ferguson & Brierley (1999)
	Upper Columbia	Millard et al. (2017)
	Upust	Gębica & Sokołowski (2002)
	Vistula and tributaries (Bren, Czarna Staszowska)	Gębica & Sokołowski (2001)
	Zohreh	Gharibreza et al. (2014)
Composite databases	—	Reynolds (1999)
	—	Millard et al. (2017)
	—	Mjøset et al. (1993)

3.2. 3D modelling and connectivity quantification

Three-dimensional gridded numerical models of idealized sedimentary architectures are produced with the scope of quantifying the influence of crevasse-splay elements on channel-body and sandbody connectivity. Two different sets of stochastic numerical models are generated, using process-based and product-oriented algorithms, respectively. Process-based modelling approaches allow for the generation of simulated sedimentary architectures that arise in response to specified geological boundary conditions and processes. Product-oriented algorithms instead aim to reproduce specified geological or geostatistical features, whose properties are defined by the user. Among these, object-based modelling algorithms generate multiple equiprobable realizations of geological architecture by placing three-dimensional bodies (objects) in a specified volume, in a way whereby inputs describing the proportions, geometry and topology of the objects are honoured.

A process-based forward model, FLUMY (v. 5.912; Cojan et al. 2004; Grappe 2014), has been applied to assess the influence of crevasse-splay elements on sandbody connectivity in the successions of meandering river systems. FLUMY simulates, in a stochastic manner, the temporal evolution of a river by mimicking processes of floodplain and streambed aggradation, and channel lateral migration, bend cut-off and avulsion; these simulated processes result in the deposition of barforms, channel fills, crevasse splays, and other overbank deposits. FLUMY operates in time steps, simulating: (i) channel-centrelines migration that varies linearly with the flow velocity near the channel banks and that is controlled by channel geometry, substrate erodibility and river slope (Ikeda et al. 1981; Lopez 2003),

(ii) channel avulsion that may take place inside or outside the simulation domain and that preferentially occurs at loci of maximum velocity perturbation, and (iii) floodplain aggradation linked to the magnitude and frequency of overbank flows (Bubnova 2018; and references therein). Although the algorithm allows for direct control over geological processes and factors, like avulsion frequency, bank erodibility, and elevation of the river equilibrium profile, these same parameters can be tuned automatically based on input values of target sand fraction, channel maximum bankfull depth, and channel-body aspect ratios (Bubnova 2018). This latter approach has been taken in this work to constrain 135 unconditional FLUMY simulations. In grids outputted by FLUMY, point-bar and channel-lag deposits are converted to a single category of sand-prone unit, whereas abandoned channel-fill deposits are treated as mud-prone. A 3x3 (planform) filter was applied to all outputs using the software TRANSCAT (Journel & Xu 1994; Remy et al. 2009); this was done to clean possible noise in the realizations, by removing isolated scattered cells of sand-prone deposits that would impact connectivity quantification (in particular the size statistics of connected components; see below).

An object-based modelling algorithm, TETRIS (Boucher et al. 2010), has been employed to create 90 unconditional object-based models of stratigraphic architectures, with the scope to determine how the presence of crevasse-splay deposits may impact channel-body connectivity in successions deposited by river systems of variable scale. The modelled stratigraphies are made of channel bodies and associated crevasse-splay elements placed in a background of overbank deposits. Channel bodies and crevasse splays are modelled as sinusoidal channelized objects and ellipsoids, respectively; the model is constrained by specifying the size distributions and proportions of these unit types, and by prescribing a relationship of adjacency between channel bodies and crevasse-splay elements. The choice of TETRIS over other object-based modelling algorithms has been made based on its ability to handle skewed distributions and to yield outputs that reflect the inputs relatively more accurately (Colombera et al. 2019).

Details on the specific inputs to both FLUMY and TETRIS are included in following sections, where the rationale for the choice of the input parameters is explained.

In modelling outputs of both FLUMY and TETRIS, the importance of crevasse-splay deposits on the static connectivity of the stratigraphic volumes is assessed by quantifying differences across two grids of the same modelling outputs in which crevasse-splay elements are coded as net or non-net volumes, respectively. This quantification is performed in terms of so-called ‘connected components’, i.e., volumes defined by clusters of cells in geocellular grids that are of the same phase (in this case, assumed net reservoir) and are connected to each other (Renard & Allard 2013). The extraction of connected components (or ‘geobodies’, hereafter) in these sets of grids has been undertaken in SGeMS (v.2.1b; Remy et al. 2009) to enable analysis of the number and size distributions of discrete compartments of net volumes. Connected components can be determined in different ways, depending on whether connectivity is considered through cell faces, edges, or corners (Pardo-Igúzquiza & Dowd 2003). In this work, the connected geobodies are determined based on full-face connectivity of grid cells; edge and corner connections are disregarded, meaning that the most conservative connectivity metrics are derived.

4. Quantification of sedimentary architectures

The connectivity of geobodies in stratigraphic successions is a function of their size, shape, proportion and spatial arrangement (cf. Hovadik & Larue 2007; Labourdette 2011; Pranter & Sommer 2011). For fluvial successions, these properties can all be characterized by outputs from FAKTS, which can therefore be used to obtain some empirical understanding of the contribution of crevasse-splay deposits to sandbody connectivity.

In FAKTS, the geometry of crevasse-splay elements is captured by records of the following attributes: (i) their maximum thickness; (ii) the width over which they extend perpendicularly away from the river channel (fill) to which they are genetically related; (iii) their down-river length measured perpendicularly to their width; and (iv) their planform area (Fig. 4A). Based on these morphometric parameters, outputs on the proportions of depositional and architectural elements in stratigraphic intervals of interest can also be extracted from FAKTS. Transitions statistics for architectural elements

can also be exported, to provide a quantitative description of how sedimentary bodies are arranged in space relative to one another, and of the extent to which sand-to-sand connectivity can be expected.

4.1. Geometries and scaling relationships

The degree to which crevasse-splay deposits contribute to the sandbody connectivity of a succession is related to the size of these elements. Hence, quantification of the geometry of crevasse-splay elements in ancient and modern analogues is presented here, for two purposes. Firstly, because some synthesis of the analogue knowledge base is useful for subsurface predictions in contexts where assessing static connectivity is important. It is common to refer to geological analogues to make predictions of the size of crevasse-splay units in subsurface successions (e.g., Lang et al. 2002; Stuart et al. 2014; Heldreich et al. 2017); quantitative knowledge of crevasse-splay geometries finds direct application for guiding well-to-well correlation in densely drilled areas and for constraining reservoir models. Secondly, results of this synthesis feed through to the numerical-modelling component of this work, by informing the choice of modelling scenarios considered for further analysis.

The distributions of morphometric parameters of the studied crevasse-splay elements display important variability, which reflects the breadth of scales of river systems considered in the database (Fig. 4). The documented crevasse-splay elements range from ca. 0.1 m to 12.0 m in thickness (mean: 1.3 m, standard deviation: 1.3 m; Fig. 4A,B), and from ca. 10 m to ca. 15 km in both cross-floodplain width (mean: 1139 m, standard deviation: 2154 m; Fig. 4A,C) and down-system length (mean: 676 m, standard deviation: 1260 m; Fig. 4A,D). Percentiles of the distributions of mean values of these parameters are, on average, larger than corresponding percentiles of the overall distributions of the parameters across all the analogues (Fig. 4B-D). This is seen because the analogue datasets dominantly exhibit positive skewness and may in part reflect how for rock-record examples some bias may exist towards smaller splay elements, which are more likely to be fully exposed in outcrop. The regional floodplain gradient can control crevasse drainage and sedimentation in a manner whereby splays may tend to be elongated in the average direction of river flow (Jorgensen & Fielding 1996; Bristow et al. 1999). Yet, the majority of the studied crevasse splays are elongated in the direction orthogonal to their parent river channel (74%, and 27% by a width-to-length ratio of two or larger; Fig. 4E), possibly because of crevasse orientation and the local gradient imposed by the accreting alluvial ridges.

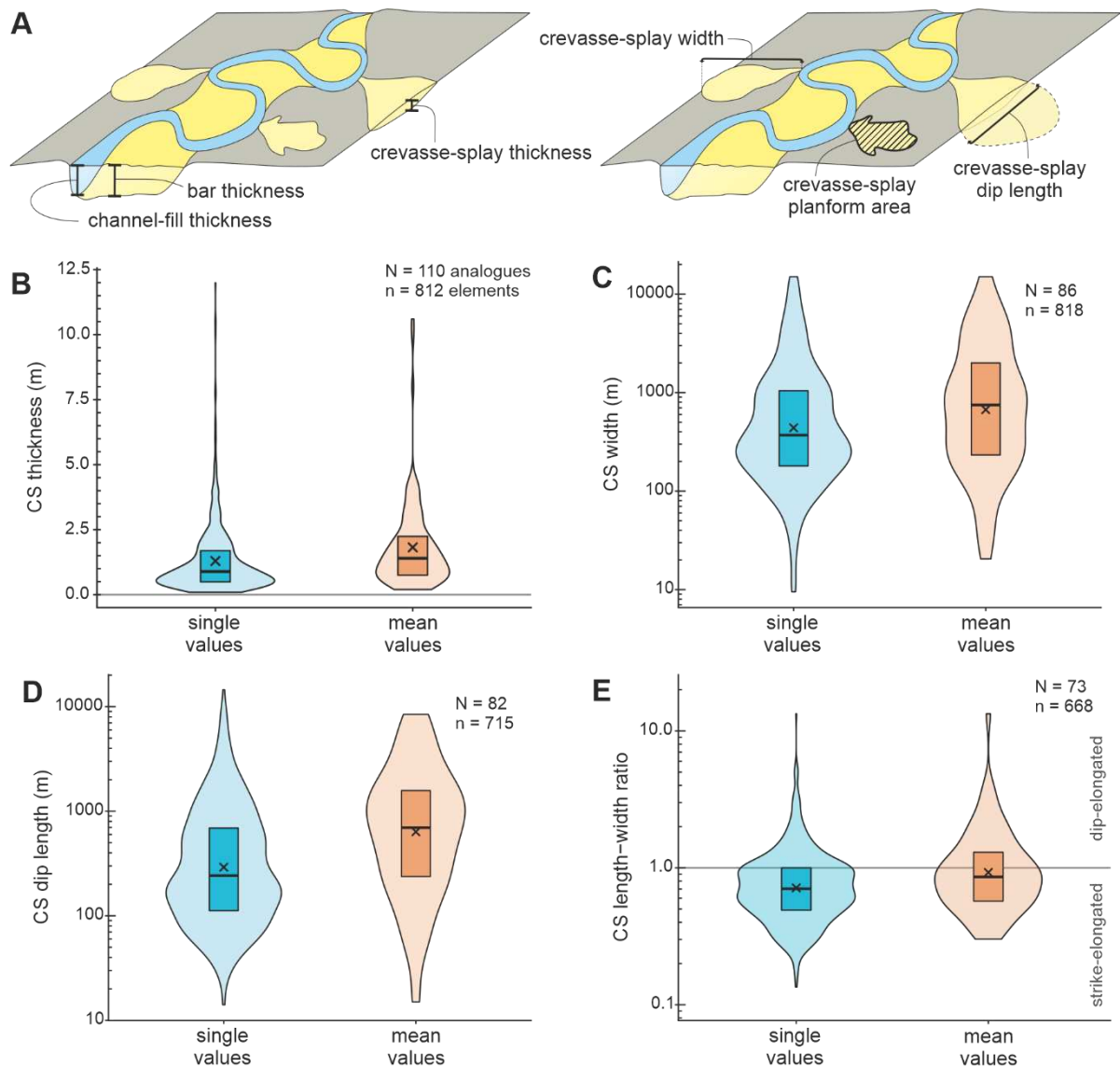


Figure 4: Morphometric parameters of crevasse-splay elements. (A) Definition diagram of parameters describing the geometry of crevasse-splay elements and associated channel elements considered in this study. (B-E) Violin plots of the distributions of crevasse-splay thickness (B), cross-floodplain width (C), dip length (D), and length-width ratio (E); distributions are presented for the entire data pool (blue) and for the mean values of every analogue (orange). CS: crevasse-splay element.

Scaling relationships between morphometric parameters of crevasse-splay elements have been assessed, since these allow prediction of likely volume and lateral correlatability of the deposits from knowledge of their thickness (cf. Mjøs et al. 1993). The geometries of crevasse-splay deposits are expected to be a function of the amount of accommodation of the floodbasin into which the splays build out and of the sediment volumes delivered by the feeder crevasses. In the dataset, overall positive scaling is seen between the thickness of crevasse-splay elements and both their width and length (Fig. 5), in agreement with previous studies (cf. Mjøs et al. 1993; Burns et al. 2017). Some moderate correlation is seen between crevasse-splay thickness and cross-floodplain splay width (data on true widths only; Pearson's $R = 0.60$, p -value < 0.001 , $N = 93$; Fig. 5A), and between values of mean thickness and mean width in stratigraphic intervals or river reaches corresponding to different sets of analogue data ($R = 0.60$, $p < 0.001$, $N = 45$; Fig. 5B). Similarly, moderate correlation is observed between crevasse-splay thickness and down-river length ($R = 0.59$, $p < 0.001$, $N = 88$; Fig. 5C), and between mean thickness and mean length in different analogue datasets ($R = 0.60$, $p < 0.001$, $N = 41$; Fig. 5D). Stronger relationships are

seen between crevasse-splay width and length (Pearson's $R = 0.83$, $p < 0.001$, $N = 668$; Fig. 5E), and between mean thickness and mean length in different analogues ($R = 0.82$, $p < 0.001$, $N = 74$; Fig. 5F). These relationships are likely to reflect how floodplain environments subject to larger and more numerous floods are expected to host splays that are, on average, both thicker and more extensive. Nevertheless, correlation between crevasse-splay thickness and planform size is relatively modest (cf. Reynolds 1999). This might be due to some variability in modes of splay construction (e.g., as dominantly aggradational vs dominantly progradational) and in the nature of floodplain accommodation. For example, a more depressed floodplain topography may accommodate splays that are comparatively thicker but more ponded and less horizontally extensive than those developed on more regular surfaces.

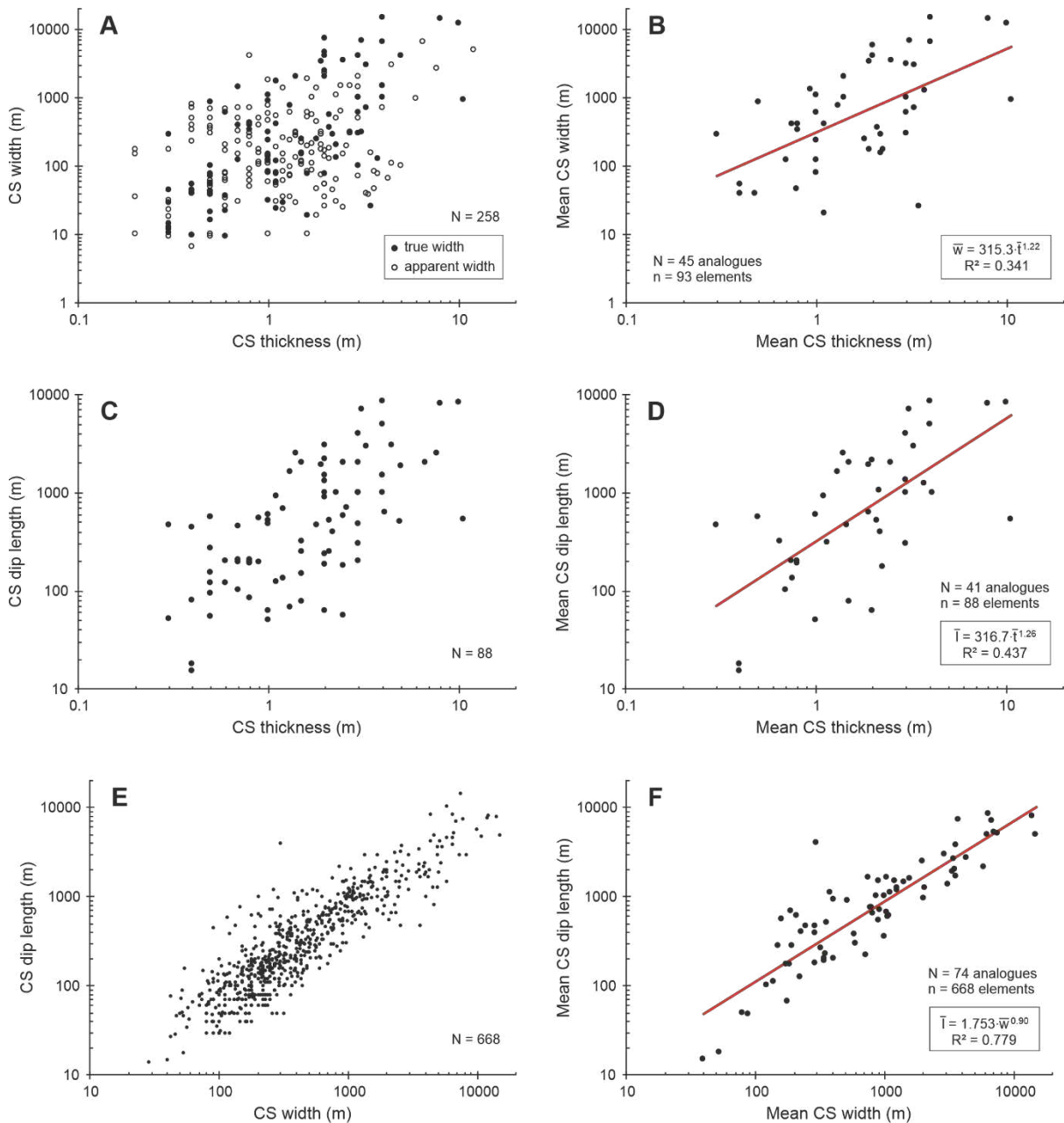


Figure 5: Scatterplots showing relationships between different morphometric parameters of crevasse-splay elements. The plots on the left-hand side contain data relating to individual crevasse-splay elements, whereas the plots on the right-hand side contain mean values for elements in analogue subsets; relationships are shown between crevasse-splay thickness and width (A) and means thereof (B), thickness and length (C) and means thereof (D), and width and length (E) and means thereof (F). CS: crevasse-splay element.

The degrees of scaling of crevasse-splay elements with the size of the river systems and of their associated channel components have also been assessed. This quantification finds application in subsurface workflows, where it can provide some constraints of geological sensibility for static models requiring channel and crevasse-splay sandbodies to be scaled realistically. Millard et al. (2017) argue that the size of a river’s drainage area may only be a secondary control on crevasse-splay size, relative to local factors relating to sediment delivery and floodplain accommodation and drainage. Furthermore, rivers with smaller drainage areas may be more prone to hydrological events that favour the transport of suspended sand onto floodplains (cf. Meybeck et al. 2003). Notwithstanding, positive scaling between catchment size and splay size is observed in the current dataset. Fairly high positive correlation is seen between the size of drainage areas upstream of the studied reaches and mean crevasse-splay thickness (Pearson’s $R = 0.84$, p -value < 0.001 , $N = 21$; Fig. 6A); moderate correlations are also seen between the logarithmic values of river catchment area and crevasse-splay width ($R = 0.67$, $p < 0.001$, $N = 39$; Fig. 6B), length ($R = 0.67$, $p < 0.001$, $N = 40$; Fig. 6C) and planform area ($R = 0.69$, $p < 0.001$, $N = 25$; Fig. 6D). These relationships can be interpreted in terms of a control by the magnitude of splay-forming floods, although the same covariance could equally arise because of larger drainage areas being typically associated with gentler river gradients on lowlands, leading to relatively increased gradient advantage over channel levees. Larger river systems may also be associated with larger floodplain accommodation, possibly because of higher rates of compaction, which could be related to the higher proportion of clays in the floodplains of lower river reaches, to an increased tendency to waterlogged conditions that may favour peat accumulation, and/or to relatively increased loading related to higher rates of sediment supply by overbank flows. Moreover, increased splay progradation further away from the levee, in response to the expected higher rates of sediment supply, could allow relatively increased vertical accretion in more distal and more depressed floodplain areas, which might also partly explain scaling in splay thickness and lateral extent (Fig. 5).

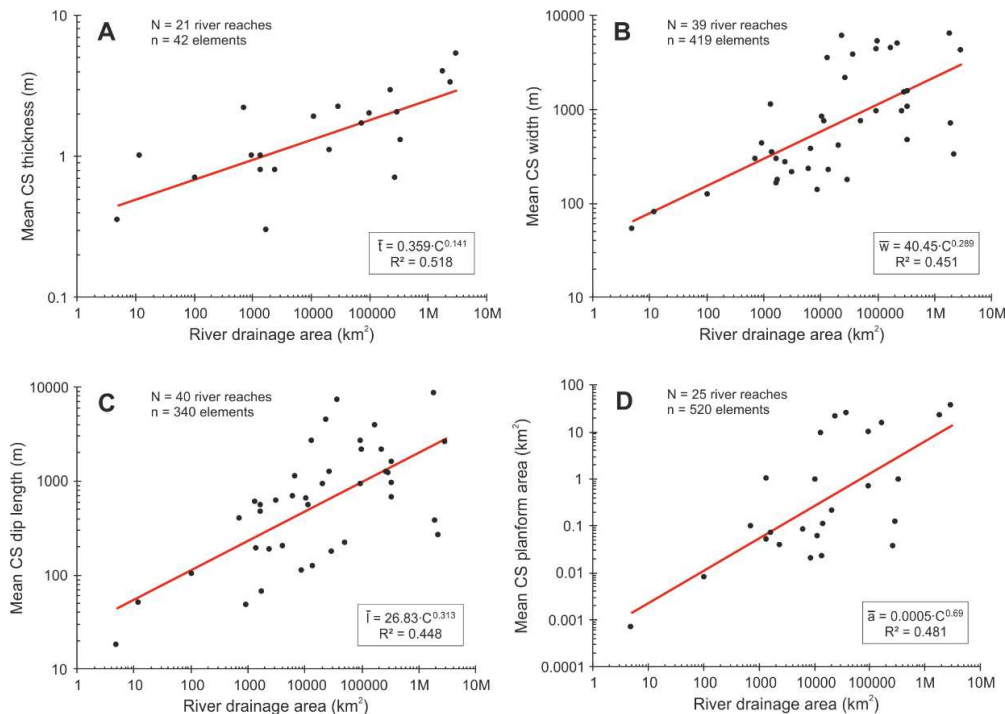


Figure 6: Scaling relationships between river catchment size and crevasse-splay morphometric parameters. Scatterplots of mean values of the thickness (A), cross-floodplain width (B), dip length (C), and planform area (D) of crevasse-splay elements against the drainage areas of the river reaches where they occur. CS: crevasse-splay element. See Supplementary Figure 1 for associated frequency distributions relative to each value of catchment size.

An assessment is also made of scaling relationships that exist between the size of crevasse splays and that of channel forms or fills (cf. Millard et al. 2017) and of channel bodies. The thickness of active or abandoned channel fills and of barform architectural elements – where these elements are fully preserved – acts as a direct measure of maximum bankfull depth. In FAKTS stratigraphic intervals and river reaches containing multiple architectural elements, moderate positive correlation is seen between the mean thickness of channel fills and the mean thickness of crevasse splays (for log-transformed values: Pearson's $R = 0.45$, p -value = 0.002, $N = 47$; Fig. 7A), and between the mean width of channels or channel fills and the mean cross-floodplain width of crevasse splays (for log-transformed values: $R = 0.63$, $p < 0.001$, $N = 60$; Fig. 7B). Where the analysis is restricted to channel and crevasse-splay elements for which lateral adjacency is recorded in the form of element transitions, slightly higher magnitude of correlation is observed between the mean thickness of channel fills or barforms and mean crevasse-splay thickness (for log-transformed values: $R = 0.70$, $p = 0.002$, $N = 17$; Fig. 7C), and between the mean width of channel or channel fills and mean crevasse-splay width (for log-transformed values: $R = 0.64$, $p < 0.001$, $N = 32$; Fig. 7D). The observed spread in the data may in part reflect the fact that overspill of suspended sediment may occur more easily across the banks of shallower channels; data on splay width and on aspect ratios expressing channel (or channel-fill) width relative to maximum bankfull depth (or thickness) demonstrate no relationship between these variables ($R = -0.124$, $N = 8$), but the dataset is small and further analysis is recommended.

In FAKTS, a channel body depositional element is a sedimentary unit made of channel deposits and with channelized geometry; a channel body can therefore represent units of different scales and hierarchies, such as a channel belt, an isolated channel fill, a portion of a valley fill, or a composite multi-storey body. Hence, these are units that are comparable to the generic channel sandbodies that are commonly incorporated in static reservoir models, and with which crevasse-splay deposits are associated in many cases (e.g., Hatløy 1994; Ma et al. 2011; Tye 2013). Quantification of the scaling between these unit types is therefore particularly useful. In FAKTS analogues, modest positive correlation is seen between the mean thickness of channel bodies and the mean thickness of crevasse-splay elements (for log-transformed values: Pearson's $R = 0.50$, p -value = 0.002, $N = 34$; Fig. 7E); stronger correlation is observed between the mean cross-stream width of channel bodies and the mean width of crevasse splays (for log-transformed values: $R = 0.85$, $p = 0.004$, $N = 9$; Fig. 7F). These relationships are likely to reflect the relative scaling between the size of the river systems and the scale of both channel-belt (cf. Xu et al. 2017) and crevasse-splay elements; in addition, however, these results may in part represent a record of how avulsion frequencies control the length of time over which processes of channel lateral migration and splay progradation may have acted. This can be considered further in the light of data on crevasse-splay element abundance.

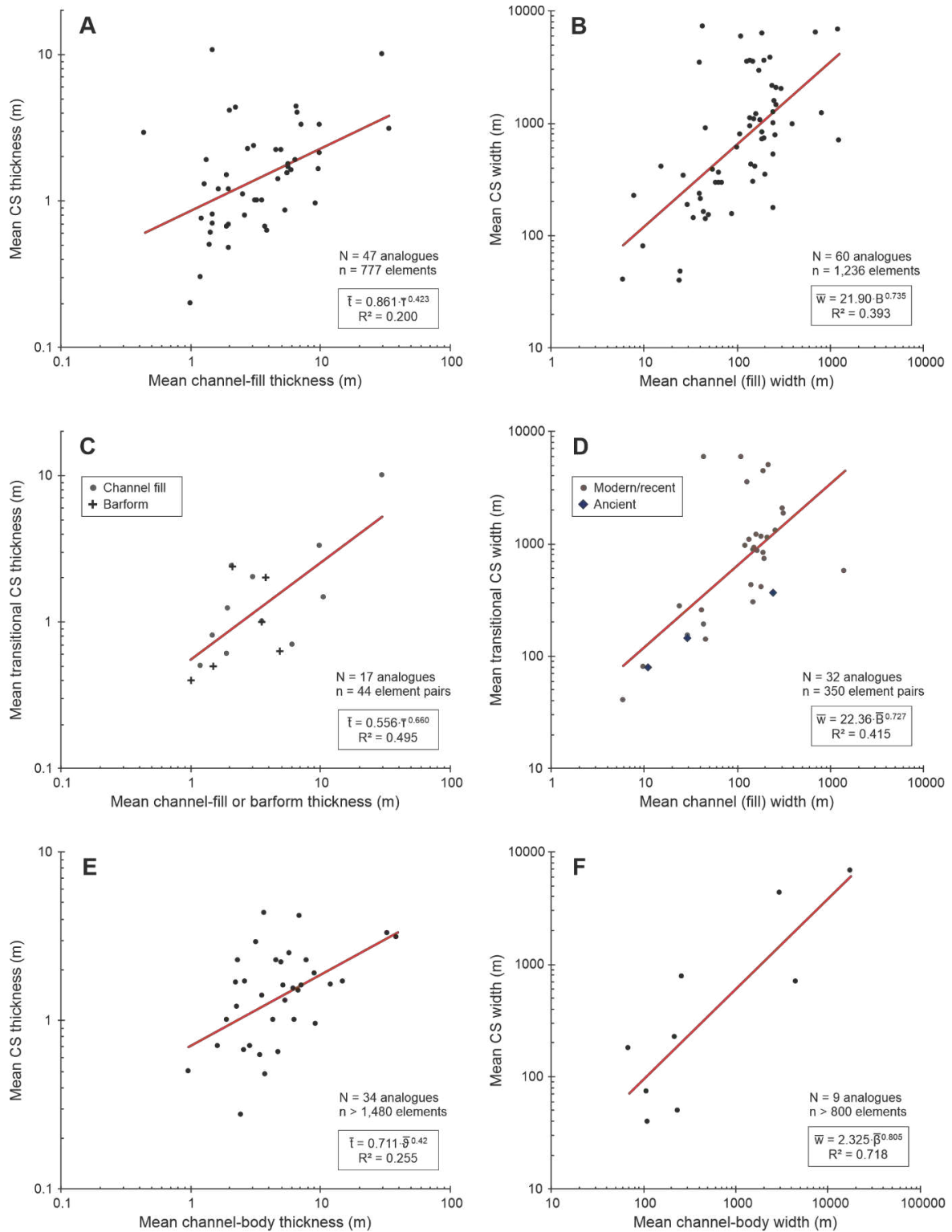


Figure 7: Scaling relationships between the size of channel elements of different types and crevasse-splay morphometric parameters. (A) Scatterplot of the mean thickness of crevasse-splay elements vs the mean thickness of channel fills contained in the same stratigraphy. (B) Scatterplot of the mean cross-floodplain width of crevasse-splay elements vs the mean width of channel forms or channel fills from the same analogues. (C) Scatterplot of the mean thickness of crevasse-splay elements vs the mean thickness of spatially related channel fills or barforms contained in the same stratigraphies. (D) Scatterplot of the mean cross-floodplain width of crevasse-splay elements vs the mean width of spatially related channel forms (modern) or channel fills (ancient or recent) from the same analogues. (E) Scatterplot of mean crevasse-splay thickness vs the mean thickness of channel bodies contained in the same stratigraphies. (F) Scatterplot of mean crevasse-splay width vs the mean width of channel bodies contained in the same stratigraphies. CS: crevasse-splay element.

4.2. Proportions of deposits

Where both channel and crevasse-splay deposits are dominantly sand-prone, their relative contribution to the overall fraction of porous volumes will control the static sandstone connectivity of a succession. Across FAKTS stratigraphic intervals suitable for derivation of element proportions and for which crevasse-splay elements are recorded ($N = 42$), the proportion of crevasse-splay deposits ranges from 1.2% to 49.7%, with a mean proportion of 11.6% (median: 8.7%; Fig. 8). In these successions, on average, crevasse-splay elements account for the 22.0% of all overbank deposits (median: 16.4%; range: 3.2% to 78.9%). Because of their close genetic relationship with channel levees, and given that some of the drivers of channel avulsion, which controls channel-body density, also influence the frequency of levee breaks (Bryant et al. 1995; Jones & Hajek 2007), the fraction of crevasse-splay elements in alluvial stratigraphies may be expected to be inherently scaled to the amount of channel deposits. Notwithstanding, in the studied stratigraphic intervals, a moderate negative relationship is seen between the proportion of channel deposits and the proportion of crevasse-splay deposits (Pearson's $R = -0.43$, p -value = 0.005, $N = 42$; Fig. 8). This is perhaps not surprising, given that the principal mechanism of reduction of the volume of overbank deposits is the erosional reworking by mobile channels, and that this process may be especially important for channel-proximal floodplain environments. This observation is also consistent with results of stratigraphic forward modelling, demonstrating that a rise in the rate of accommodation generation can set the conditions (e.g., gradient advantage) that drive an increase in the proportion of crevasse-splay deposits, and that this occurs simultaneously with a decrease in the fraction of channel deposits (Edington 2003; Edington & Poeter 2006). The same observation could also be interpreted in terms of how longer interavulsion periods may facilitate the formation of crevasse splays, by allowing longer times for levee aggradation and splay growth. Nevertheless, a modest positive relationship is instead seen between the proportion of channel deposits in the studied stratigraphies and the fraction of overbank deposits made of crevasse-splay sediments (Pearson's $R = 0.33$, p -value = 0.030, $N = 42$; Fig. 8), and this observation can be explained by the anticipated intimate relationship between processes of channel and splay sedimentation.

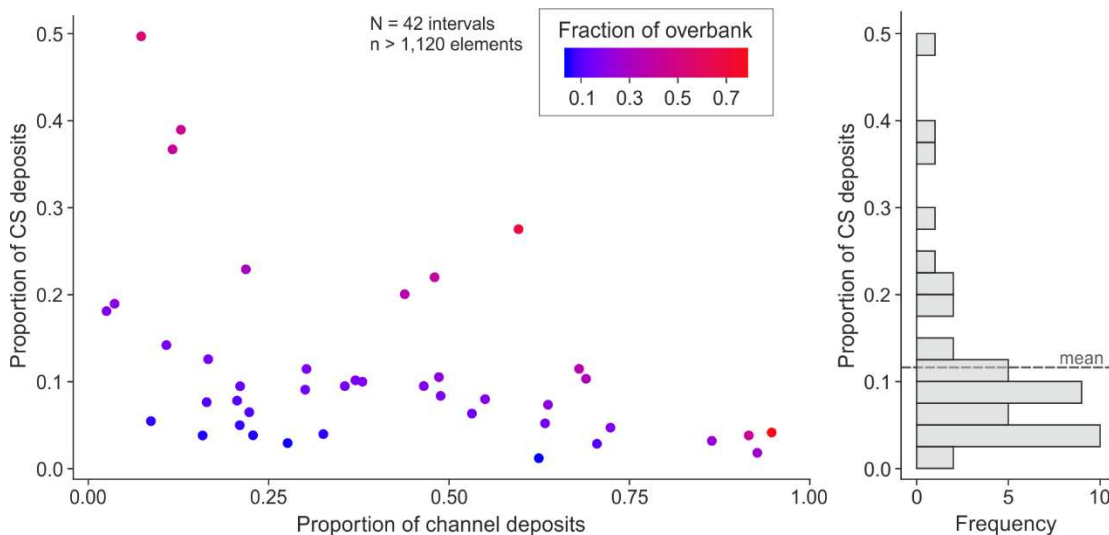


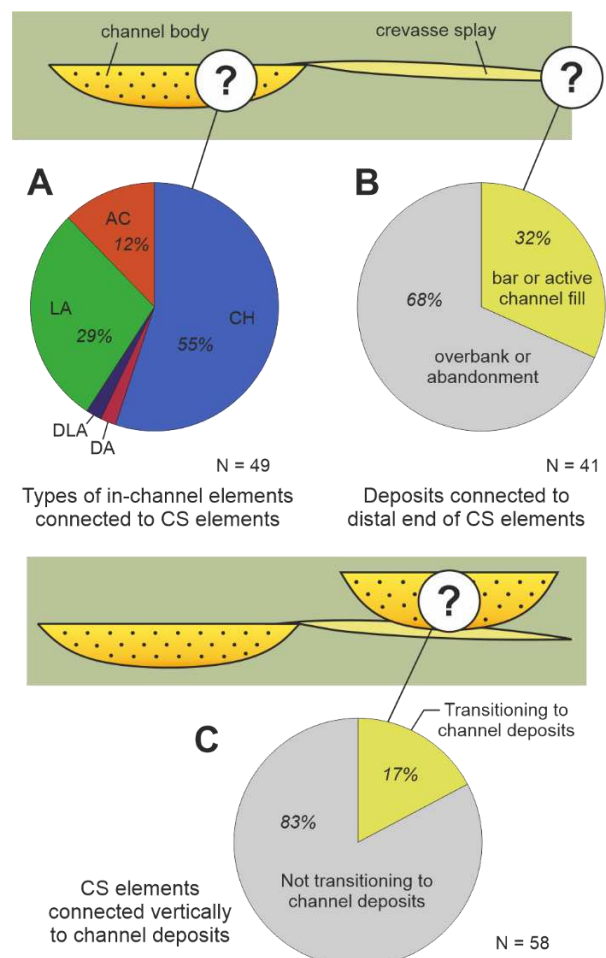
Figure 8: Analogue data on the proportion of crevasse-splay and channel deposits in stratigraphic volumes. The scatterplot shows the proportion of crevasse-splay elements vs the proportion of channel deposits in the same analogue, colour-coded according to the fraction of total overbank deposits made of crevasse-splay elements. CS: crevasse-splay element.

4.3. Transition statistics

The origin of the channel deposits to which crevasse-splay elements are seen to be physically connected determines their likely lithology, and so the likelihood of development of sandbody communication across channel and overbank environments, and across separate channel bodies. The vertical and lateral arrangement of neighbouring channel and crevasse-splay deposits determines the degree to which the presence of splay elements may typically enhance sandbody connectivity vertically and laterally (Fig. 2B). These characteristics in the spatial arrangement of sedimentary units in fluvial strata are quantified here using FAKTS output from outcrop-analogue datasets suitable for deriving transitions statistics of architectural elements.

The lithology of in-channel architectural elements can vary significantly, yet some general considerations can be made. Of all FAKTS crevasse-splay elements for which transitions statistics can be extracted, ca. 12% emanate from abandoned channel fills, which typically take the form of mud plugs or heterolithic fills (Fig. 9A). Approximately 29% of crevasse splays are instead seen to transition laterally to lateral-accreting barforms, such as point bars (Fig. 9A); these may contribute in a limited way to sand connectivity, if developed on top of, or away from, mud-prone bar tops that are typical of point-bar elements (cf. Yan et al. 2019). Away from their genetically related channel bodies, 32% of the crevasse-splay elements are seen to transition laterally into active channel deposits, rather than pinching out into overbank mudstones (Fig. 9B). Ca. 17% of the splay elements are seen to transition vertically to channel bodies that have partially eroded them (Fig. 9C). Assuming all active-channel deposits to be sand-prone and all abandonments to form mud plugs, the overall probability of a crevasse-splay element to act as a connector between different channel sandbodies is 0.28 and 0.15, for channel bodies stacked laterally or vertically, respectively. These quantities give a sense of what might be typical in fluvial successions, but will vary significantly as a function of the channel-body density within the stratigraphic package being characterized, and of the channel subenvironments it records.

Figure 9: Database outputs on transitions statistics of crevasse-splay and associated channel elements. (A) Relative frequency of channel architectural-element types connected with crevasse-splay elements. AC: abandoned channel fill; CH: aggradational channel fill; DA: downstream-accreting macroform; DLA: downstream and/or lateral accreting macroform; LA: lateral-accretion macroform (see Colombera et al. 2013). (B) Frequency with which crevasse-splay elements transition to sand-prone channel elements laterally away from their associated channel deposits. (C) Frequency with which crevasse-splay elements tend to be overlain by channel deposits. CS: crevasse-splay element.



5. Quantification of connectivity in stochastic models

5.1. Process-based models

5.1.1. Modelling rationale and inputs

A set of 135 numerical stratigraphies has been simulated using FLUMY (Grappe et al. 2016) to assess the influence of crevasse-splay elements on sandbody connectivity in fluvial successions deposited by meandering rivers. In these simulations, it has been assumed that point-bar, thalweg and crevasse-splay elements form sand-prone units, that these units sit in a background of overbank fines, and that they are compartmentalized by abandoned-channel fills (mud plugs; Fig. 2C).

FLUMY simulations have been constrained by input parameters describing the following: (i) maximum channel bankfull depth; (ii) sandbody extension index (i.e., a measure of the lateral extent of the accumulated channel belts, expressed in terms of meander amplitude and relative to the channel depth; Bubnova 2018); and (iii) target net-to-gross ratio. Each of these parameters has been set as taking three alternative values, as reported in Table 2. As a result, twenty-seven (3^3) different combinations of input parameters have been considered overall, and five synthetic stratigraphies have been generated for each combination of input parameters, for a total of 135 simulations. The modelled domain is a cuboidal Cartesian grid. The thickness of each modelled stratigraphic volume corresponds to five times the depth of the formative river, and hence ranges from 5 m to 75 m. The model domain covers a square planform area, which is scaled to the values of both river size and sandbody extension index, and ranges from 0.49 km² to 400 km² (Table 2). Depending on the chosen inputs (Table 2), to achieve the required amount of floodplain aggradation, the simulations have been performed over ca. $1.5 \cdot 10^4$ to $1.0 \cdot 10^5$ iterations, which are time steps over which the processes of river migration and avulsion are modelled. The proportion and size of crevasse-splay deposits cannot be controlled directly, as they result instead from the simulated river morphodynamics, as explained in section 3.2.

Table 2: Input parameters employed in FLUMY and chosen input values. A constant channel width-to-depth ratio of 10.0 has been selected for all the simulations. All possible combinations of these parameters (3^3) define the twenty-seven sets of simulations run in this study.

FLUMY parameter	Parameter description	Input values
Dmax (m)	Channel maximum bankfull depth	1, 5, 15
Isbx (-)	Sandbody extension index	20, 80, 110
NTG (%)	Target net-to-gross ratio	20, 40, 60
Grid length (m)	Downdip length of grid	[700–20,000]
Grid width (m)	Along-strike width of grid	[700–20,000]
DX (m)	Downdip grid resolution	[3–25]
DY (m)	Along-strike grid resolution	[3–25]

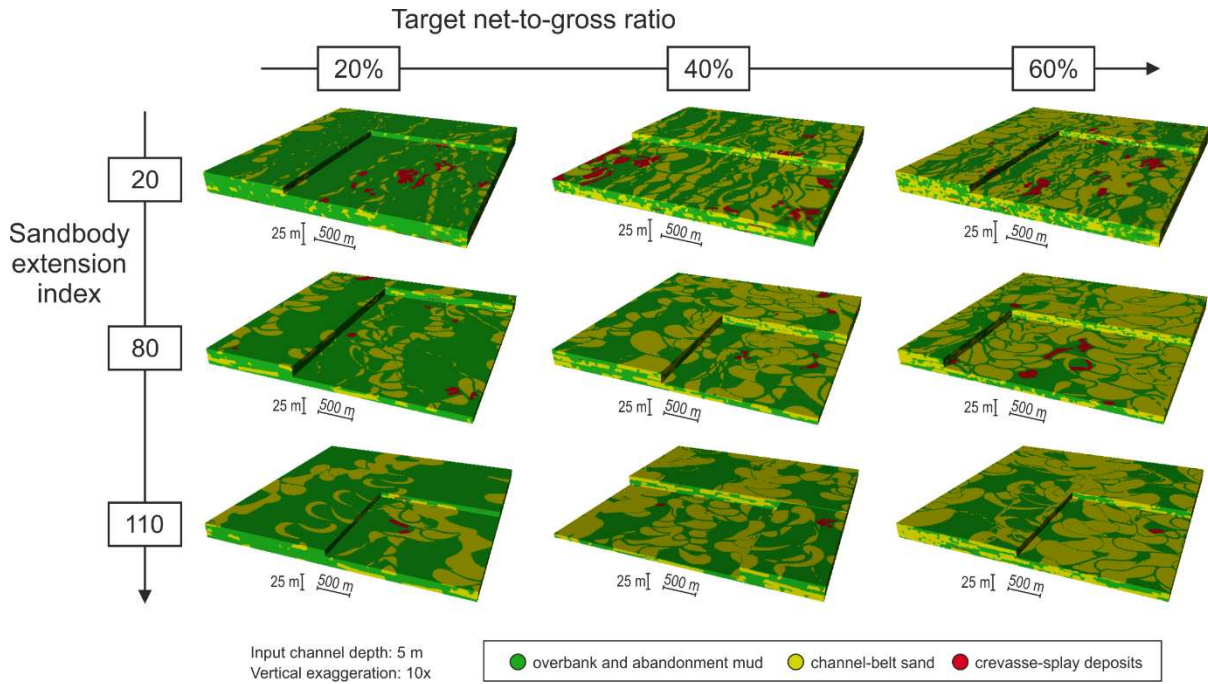


Figure 10: Example FLUMY outputs for different input values of target net-to-gross ratio and sandbody extension index. The grids are coded so as to distinguish channel (point-bar and channel-fill) sandbodies, overbank and channel-fill muds, and crevasse-splay elements. Nine examples are shown here from the total of 135 simulations. These nine examples are associated with an input channel depth of 5 m; additional sets of simulations have been run with channel depths of 1 and 15 m to define twenty-seven scenarios in total (see Table 2).

5.1.2. Outputs and connectivity analysis

All FLUMY realizations have been processed so as to distinguish crevasse-splay and crevasse-channel deposits from channel-belt sandbodies (Fig. 10), allowing for a quantitative evaluation of the importance of crevasse-splay deposits on sandbody connectivity under different conditions of net-to-gross ratio and channel-belt size (see section 3.2).

Across all the realizations, the proportion of crevasse-splay deposits varies between 0.1% and 1.8%, with an average of 0.5% (Fig. 11C-D). The fraction of crevasse-splay deposits increases, on average, for a decrease in input sandbody extension index, whereas it does not vary systematically with the target net-to-gross ratio. It is likely that these results reflect how, in order to attain a given net-to-gross ratio, stratigraphies containing narrower channel bodies, must embody a larger number of channel threads, themselves arising from more frequent avulsions. The relatively higher proportion of crevasse-splay deposits can be explained by the higher density of (i) channel threads, from which crevasse splays can originate, and (ii) of avulsion nodes, to which some splays may be genetically related.

In the grids, with the inclusion of crevasse-splay deposits as net volumes, the number of geobodies (whether simple or compound in type) will remain constant, decrease, or increase, depending on the frequency with which these splay units are connected to a single channel sandbody, to two or more channel sandbodies, or exclusively to mud plugs, respectively. These same situations, together with the size distribution of the crevasse-splay units, will also control how the size of the connected geobodies varies in response to the inclusion of the splay deposits. Thus, the number and size of connected geobodies describes: (i) the degree to which sand volumes in a fluvial succession become more compartmentalized, where sandy splays are only connected to mud plugs; and (ii) the degree to which sand volumes might become more widely connected, due to primary or secondary connectivity between crevasse splays and sand-prone channel deposits. The modelled Cartesian grids take three different values of specific surface area, associated with the three input values of channel depth to which the grids are scaled. No significant difference is seen in the distributions of these metrics across the three

values of specific surface area; therefore, distributions of the studied metrics associated with these different grid geometries are considered jointly for further analysis (Fig. 11).

The only set of realizations for which the inclusion of crevasse-splay deposits results in increased sandbody connectivity is that associated with the smallest value of sandbody extension index, i.e., those that incorporate the narrowest channel bodies (relative to the depth of their formative rivers). In these realizations, a decrease in the number of geobodies is seen for those with a target net-to-gross ratio of 40% and 60% and for approximately half (7 out of 15) of those with a 20% target (Fig. 11A). An increase in the average size of the geobodies is also seen in all the realizations in this group (Fig. 11B). The magnitude of this increase in connectivity tends to be scaled directly with the target net-to-gross value (Fig. 11A-B), which itself correlates with the proportion of crevasse-splay deposits (Fig. 11C-D). Instead, for outputs with more laterally extensive channel belts, the addition of crevasse-splay deposits – albeit increasing the overall sandbody volume – makes the stratigraphy more compartmentalized on average, in spite of the fact that these realizations are characterized by a total sand fraction that is larger and typically exceeding the target value by a significant margin (Fig. 11E-F). This may be due to the reduced likelihood of secondary connections caused by channel reworking, since these outputs are characterized by more widely spaced channel bodies and wider intervening floodplain packages, themselves containing a smaller fraction of crevasse-splay deposits, relative to realizations associated with narrower channel bodies (Fig. 10; Fig. 11D). More generally, in sets of simulations with any channel-body geometry, the degree of compartmentalization increases, in relative terms, as the target net-to-gross ratio decreases (Fig. 11A,B,F); this fact can again be interpreted in terms of a progressive reduction in the amount of secondary connectivity, which can be attributed to more limited overbank cannibalization by channels that are less mobile. In summary, mud-plug compartmentalization of crevasse-splay sands appears to be more important for successions in which channel-body width-to-thickness aspect ratios are larger and net-to-gross ratios are smaller.

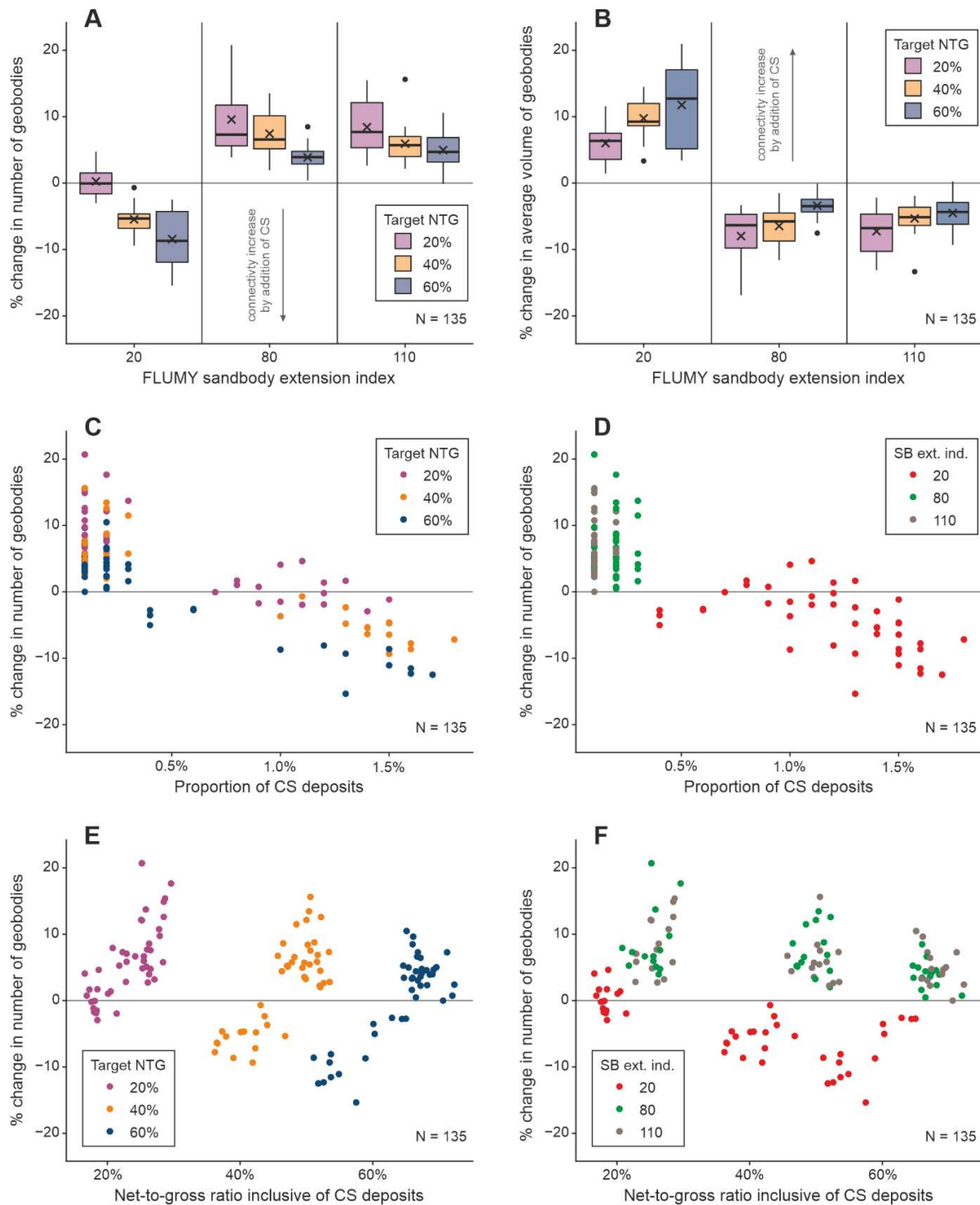


Figure 11: Quantitative evaluation of FLUMY outputs, illustrating connectivity variations in relation to the inclusion of crevasse-splay elements in the modelling grids. (A-B) Boxplots showing distributions in the relative change (expressed in percentage) in the number of geobodies (A) and in the average geobody volume (B) for different sets of simulations grouped by target net-to-gross ratio and sandbody extension index. Boxes represent interquartile ranges, horizontal bars in boxes represent medians, crosses (x) represent mean values, and spots represent outliers. (C-D) Scatterplots showing the relative change (in percentage) in the number of geobodies vs the proportion of crevasse-splay deposits, colour-coded by target net-to-gross ratio (C) and sandbody extension index (D). (E-F) Scatterplots showing the relative change (in percentage) in the number of geobodies vs the effective net-to-gross ratio (considering crevasse-splay deposits as net volumes), colour-coded by target net-to-gross ratio (E) and sandbody extension index (F). If separate channel sandbodies become connected by splay elements, the number of connected geobodies decreases, whereas the average geobody size increases. CS: crevasse-splay element; NTG: net-to-gross ratio.

5.2. Object-based models

5.2.1. Modelling rationale and inputs

A series of 90 unconditional object-based geocellular models has been built using TETRIS (Boucher et al. 2010), with the scope to derive knowledge that can help reduce uncertainty as to how the presence of crevasse-splay deposits may impact channel-body connectivity in successions deposited by river systems of different scales. To this end, inherent scaling relationships between channel and crevasse-splay deposits can be used: by knowing the way in which values of thickness, width, amplitude and wavelength of channel sandbodies tend to scale with each other, and how the size of crevasse-splay elements tends to scale relative to that of channel bodies, it ought to be possible to make some predictions of how the presence of crevasse-splay deposits may typically control the interconnectedness of channel bodies in successions of river systems of different sizes and net-to-gross ratios. This modelling effort allows determination of the contribution of crevasse-splay deposits to variations in channel-body connectivity. Specifically, it enables consideration of how static connectivity may relate to (i) the variable scaling of the geometric parameters of the modelled objects and (ii) to a realistic range of proportions of crevasse-splay deposits. The results can also be used to predict the static connectivity of object-based models built on alternative inputs constrained by sensible distributions of element sizes. The modelling is undertaken with the expectation that results will be representative of what may be typical for fluvial successions. However, it is acknowledged that variability in the morphometric scaling of sedimentary units is significant (Figs. 5-7; Colombera et al. 2019). Also, a gross simplification is made whereby connectivity is evaluated for crevasse-splay elements and channel bodies that are assumed to be internally homogeneous; thus, this approach ignores lithological heterogeneity determined by internal lithological organization (Fig. 2A).

To constrain the object-based models, three scenarios of river-system scale are considered that cover the broad range of channel-body and crevasse-splay sizes recorded in the FAKTS database. Based on the analysis of 122 analogue stratigraphic volumes from FAKTS, containing at least ten channel bodies each and 4,445 in total, a distribution of mean values of channel-body thickness in the analogues is obtained that is characterized by fifth, fiftieth (median) and ninety-fifth centiles taking the following values: 2.1 m, 5.7 m, 18.0 m. These values define the mean thickness of channel bodies in the modelled architectures, and three corresponding scenarios of river-system scale. Reference values of river-system size are determined based on the positive scaling between mean channel-body thickness and river drainage area, as seen in FAKTS analogues (Supplementary Figure 2A; cf. Xu et al. 2017). Corresponding values of river catchment size are considered to define input mean values of channel-body width, and of crevasse-splay thickness, width and length, based on empirical relationships compiled using FAKTS analogues (Supplementary Figure 2B; Fig. 6). Additional empirical relationships based on FAKTS analogues, compiled by Colombera et al. (2019), are applied to derive the following: (i) input values of mean channel-body amplitude and wavelength, which have been scaled to the mean channel-body width; and (ii) input values of standard deviation in channel-body thickness, width, amplitude, and wavelength, which have been scaled to their respective means. Similar empirical relationships are used to define input values of standard deviation in crevasse-splay thickness, width and length (Supplementary Figure 3). All geometric parameters have been assigned lognormal distributions, in consideration of positive skewness being dominantly recognized in corresponding distributions in the studied analogues (cf. Colombera et al. 2019). Channel and crevasse-splay deposits are both considered as contributing to net volumes, and two sets of models have been constrained assuming the total net-to-gross ratio as taking values of 20% and 40%. Unlike for the FLUMY simulations, scenarios associated with a 60% net-to-gross ratio were not considered, since under these conditions channelized architectures tend to be highly connected, statically, in any case (Larue & Hovadik, 2006). The relative fraction of channel and crevasse-splay deposits that make up these volumes is assumed to vary according to three proportions of crevasse-splay elements, reflecting the twenty-fifth, fiftieth (median) and seventy-fifth centiles of their proportions in FAKTS analogues (Fig. 8); these correspond to relative fractions of 5%, 9% and 12%, respectively (Fig. 12). In total, 18 different parameter sets arise from the combination of scenarios of river-system size, net-to-gross ratio and crevasse-splay fraction; five equiprobable realizations are produced for each scenario, for a total of 90 grids. The modelled domains are cuboidal Cartesian grids scaled to the three scenarios of river-system

size, with thickness ranging from 25 m to 100 m, and with a square planform area ranging from 36 km² to 1,024 km². The parameters used to constrain the TETRIS models are summarized in Table 3.

Table 3: Input parameters used to constrain the 18 sets of TETRIS models . All geometric parameters are scaled relative to the mean channel-body thickness, defining three scenarios of river-system scales that are separately shown under three subcolumns of column ‘Input values’. CS = crevasse-splay element; St. Dev. = standard deviation.

TETRIS parameter	Parameter definition	Input values		
NTG (%)	Net-to-gross ratio, defined as the sum of the proportion of channel and crevasse-splay deposits	20, 40		
Proportion of CS deposits (%)	25 th , 50 th and 75 th centiles of the distribution of proportions of crevasse-splay deposits (Fig. 8)	5, 9, 12		
Mean channel-body thickness (m)	5 th , 50 th and 95 th centiles of the distribution of channel-body thickness in FAKTS analogues	2.1	5.7	18.0
Channel-body thickness st. dev. (m)	Established based on mean channel-body thickness (see Colombera et al., 2019)	1.3	3.3	9.7
Mean channel-body width (m)	Established based on mean channel-body thickness using relationships in Supplementary Figure 2	530	1387	4189
Channel-body width st. dev. (m)	Established based on mean channel-body width (see Colombera et al., 2019)	428	1175	3751
Mean channel-body wavelength (m)	Established based on mean channel-body width (see Colombera et al., 2019)	4513	8675	18399
Channel-body wavelength st. dev. (m)	Established based on mean channel-body wavelength (see Colombera et al., 2019)	3692	7188	15357
Mean channel-body amplitude (m)	Established based on mean channel-body width (see Colombera et al., 2019)	436	969	2425
Channel-body amplitude st. dev. (m)	Established based on mean channel-body amplitude (see Colombera et al., 2019)	445	1020	2650
Mean CS thickness (m)	Established based on river-system scale using relationship in Figure 6A	1.0	1.4	2.1
CS thickness st. dev. (m)	Established based on mean CS thickness using relationship in Supplementary Figure 3	0.5	0.8	1.3
Mean CS width (m)	Established based on river-system scale using relationship in Figure 6B	351	681	1464
CS width st. dev. (m)	Established based on mean CS width using relationship in Supplementary Figure 3	209	404	863
Mean CS dip length (m)	Established based on river-system scale using relationship in Figure 6C	278	572	1308
CS dip length st. dev. (m)	Established based on mean CS length using relationship in Supplementary Figure 3	173	372	902
Grid height (m)	Height of cartesian grid	[25-100]		
Grid area (km ²)	Square planform area of cartesian grid	[36-1,024]		
DZ (m)	Vertical grid resolution	[0.25-1.00]		
DX (m)	Downdip grid resolution	[15-160]		
DY (m)	Along-strike grid resolution	[15-160]		

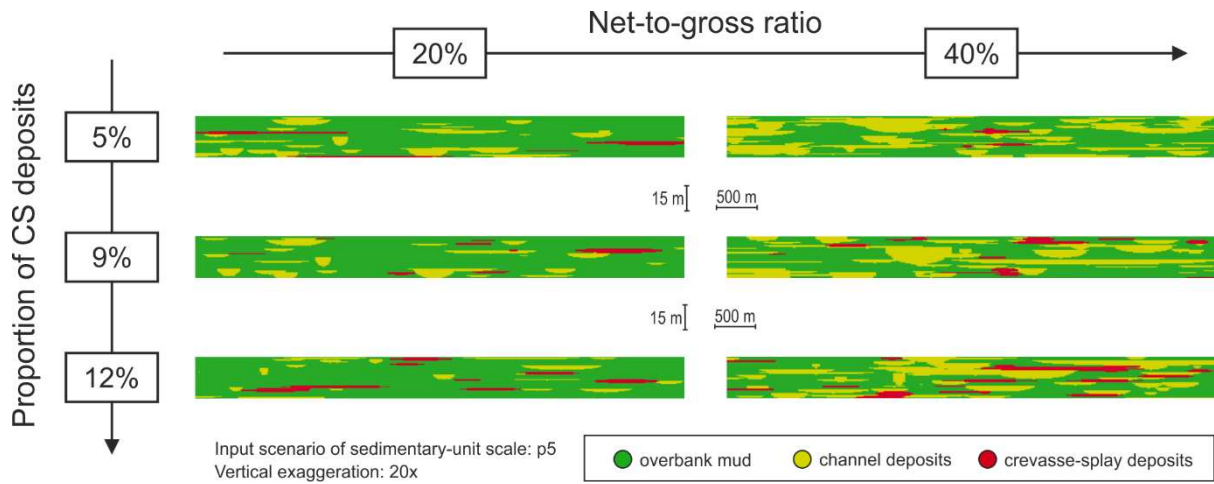


Figure 12: Vertical cross-sections through example TETRIS outputs, obtained for different input values of net-to-gross ratio and proportion of crevasse-splay deposits. Channel-body elongation is perpendicular to the view. These six examples are associated with the scenario of river-system scale corresponding to the 5th centile of channel-body thickness; additional sets of simulations have been run for river-system scales associated with the 50th and 95th centiles, to define eighteen scenarios in total (see Table 3).

5.2.2. Outputs and connectivity analysis

The influence of crevasse-splay deposits on the static connectivity of the realizations is again considered in terms of relative changes in the number and volume of connected geobodies caused by the inclusion of splay elements in the grids (Fig. 13 and Supplementary Figure 4). Because the splays are invariably attached to the channel bodies, their incorporation in the grids normally returns a reduction in the number of geobodies, with the exception of six grids for which this quantity does not change (i.e., six cases in which none of the splay elements acts to connect otherwise disconnected channel bodies) (Fig. 13A). Overall, the connectivity growth becomes less marked as the scale of channel bodies and crevasse splays increases across the three scenarios (which are also associated with a decrease in grid specific area); however, differences in the mean values of connectivity metrics across the three groups are not statistically significant when tested by analysis of variance, neither for the relative change in the number of geobodies (Welch's one-way ANOVA: $F[2, 56.55] = 1.23$, p -value = 0.301), nor for the relative change in their average ($F[2, 52.53] = 1.09$, $p = 0.345$) or maximum ($F[2, 56.22] = 0.50$, $p = 0.612$) volume.

In relative terms, the connectivity increase is more important for the series of realizations with 20% net-to-gross ratio; differences in the relative change in geobody size between this set of outputs and the 40% net-to-gross group are statistically significant, when evaluated for both average (Welch's test: $F[1, 56.63] = 6.06$, $p = 0.017$) and maximum geobody volumes ($F[1, 55.32] = 9.50$, $p = 0.003$). Over the entire dataset ($N = 90$), the relative contribution of crevasse-splay deposits to the net-to-gross ratio exhibits (i) a weak but statistically significant negative correlation with the relative change in the number of connected geobodies (Pearson's $R = -0.25$, p -value = 0.018), and (ii) a modest positive correlation with the relative changes in average ($R = 0.49$, $p < 0.001$) and maximum ($R = 0.28$, $p = 0.007$) geobody volume (Fig. 13C). These results are expected, since a more substantial addition of net volumes should translate to a larger relative change in connectivity metrics. However, the relationship between the growth in connectivity and the relative increase in net-to-gross ratio varies across the different sets of realizations. In particular, in the series of outputs with the lower input net-to-gross ratio (20%), this change in connectivity is especially evident for realizations associated with the scenario of smallest fluvial systems, and is instead not recognized in those related to the largest-scale systems (Fig. 13A).

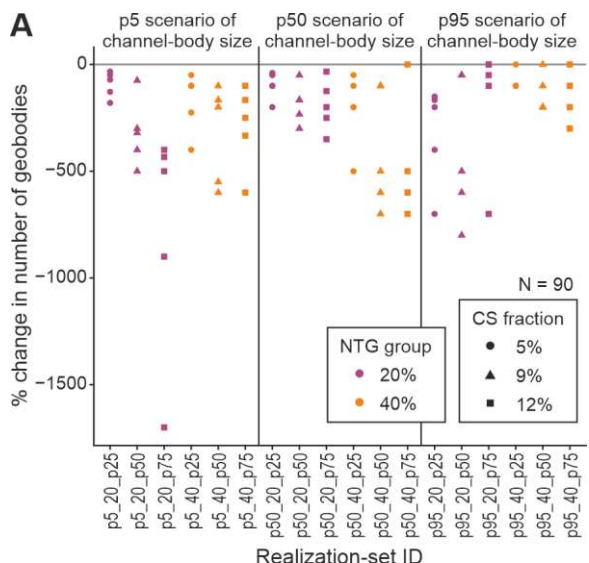
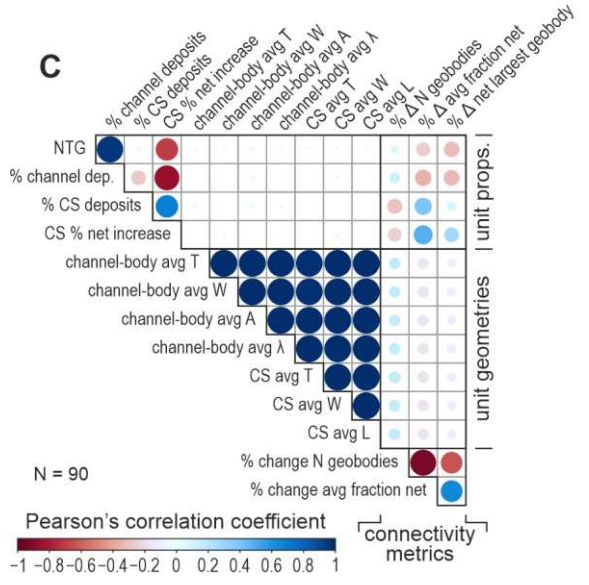
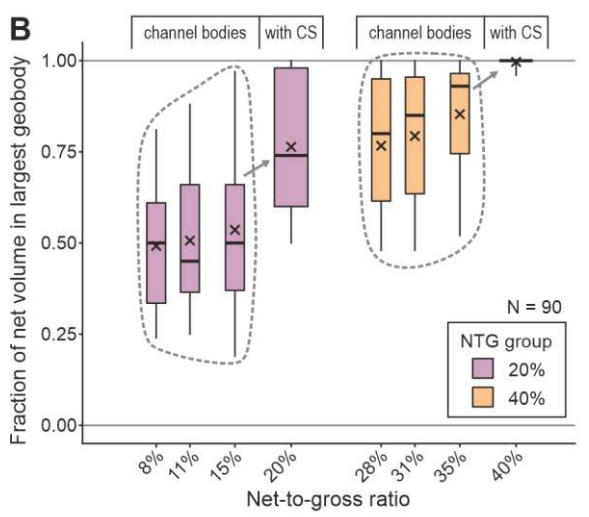


Figure 13: Quantitative evaluation of TETRIS outputs, illustrating connectivity variations in relation to the inclusion of crevasse-splay elements in the modelling grids. (A) Dotplots showing distributions in the relative change (expressed in percentage) in the number of geobodies for different sets of simulations grouped by target net-to-gross ratio, fraction of crevasse-splay deposits, and scenario of river-system scale. (B) Boxplots showing distributions in the fraction of net volumes contained in the largest connected geobody, for different sets of simulations grouped by effective net-to-gross ratio; metrics associated with grids containing channel bodies only vs grids containing channel and crevasse-splay elements are presented separately. Boxes represent interquartile ranges, horizontal bars in boxes represent medians, and crosses (x) represent mean values. (C) Correlation matrix of model inputs of sedimentary-unit geometries and proportions and extracted connectivity metrics; see also Supplementary Figure 4. CS: crevasse-splay element.



In grids in which splays are not incorporated, the proportion of channel deposits (which varies over six values, from 8% to 35%) shows moderate negative correlation ($R = -0.45$, $p < 0.001$) with the absolute number of geobodies, taking average values of 8.7 and 4.8 for the sets of models with lower and higher net-to-gross ratios, respectively. This indicates that, despite the fact that the channelized units are modelled as separate unrelated units (meaning that connectivity cannot be controlled by the presence of avulsion nodes or tributary or distributary patterns), an increase in their number still reduces the average number of geobodies by driving channel-body amalgamation. Differences in connectivity are apparent between these channelized architectures (i.e., realizations in which splay deposits are not included) and the mixed architectures of grids that incorporate both channel bodies and splays, with the latter achieving, on average, the same level of static connectivity of the largest geobody for a smaller value of net-to-gross ratio. Specifically, the average fraction of net volume contained in the largest connected geobody is comparable for mixed architectures with a net-to-gross ratio of 20% and channelized architectures with ca. 30% net-to-gross (Fig. 13B), although in this latter group the largest geobodies will necessarily tend to be larger in absolute volume. When crevasse-splay elements are added to the set of realizations with higher net-to-gross ratios, to reach the 40% target, full or nearly full connectivity is always achieved across the grids (over 95% of the net volumes are contained in a single geobody; Fig. 13B).

Overall, assuming some typical scaling between the sedimentary units, the role of crevasse splays as connectors of channel bodies seems more important for smaller fluvial systems and for lower net-to-gross ratios. Moreover, the occurrence of splays results in architectures that may be as broadly connected as purely channelized architectures with larger net volumes.

6. Summary and discussion

Crevasse-splay deposits are common components of subsurface fluvial successions, for which static-connectivity predictions are needed in a variety of applications, including hydrocarbon production, exploitation of geothermal heat, underground carbon capture and storage, prediction of contaminant dispersion, and aquifer use and remediation (e.g., Hardage et al. 1996; Ambrose et al. 2008; Burns et al. 2010a,b; Mastrocicco et al. 2011; Hansen et al. 2013; Lew et al. 2016; El-Mowafy & Marfurt 2016; Willems et al. 2017; Dall'Alba et al. 2020).

Together with their lithology, the size, proportion and topology of crevasse-splay bodies will determine the sandbody connectivity of the fluvial successions in which they are contained. The analyses of the analogue data and of the modelling outputs demonstrate how these properties vary in nature, and the manner in which they control connectivity, at least under some conditions and where crevasse splays form effective porous media. Based on the recognized architectural styles, the role of crevasse-splay elements in the connectivity of fluvial successions can be categorized into three situations (Fig. 14), which can arise due to primary and/or secondary connections (see section 2), and which can be summarized as follows.

- *Crevasse splays that form isolated compartments.* This situation may occur for example where splays are physically adjacent (and commonly genetically linked) to mud plugs; it may be common in low net-to-gross successions of meandering river systems, as indicated by the process-based modelling study presented in this work (section 5.1).
- *Crevasse splays that are connected to single channel sandbodies.* This architectural configuration is characterized by composite sandbodies that are necessarily larger in size than the channel bodies alone. Their larger planform area makes intersection of sandbodies by a vertical well more likely. However, the presence of splay bodies determines a limited increase in the size of connected geobodies. Analogue data suggest that this may be the most common situation (section 4.3).
- *Crevasse splays that are connected to two or more channel sandbodies.* This architecture results in a broader increase in vertical and/or horizontal connectivity through the stratigraphy but may only be common in high net-to-gross successions, in which channel bodies may already be connected because of amalgamation (cf. sections 4.3, 5.2).

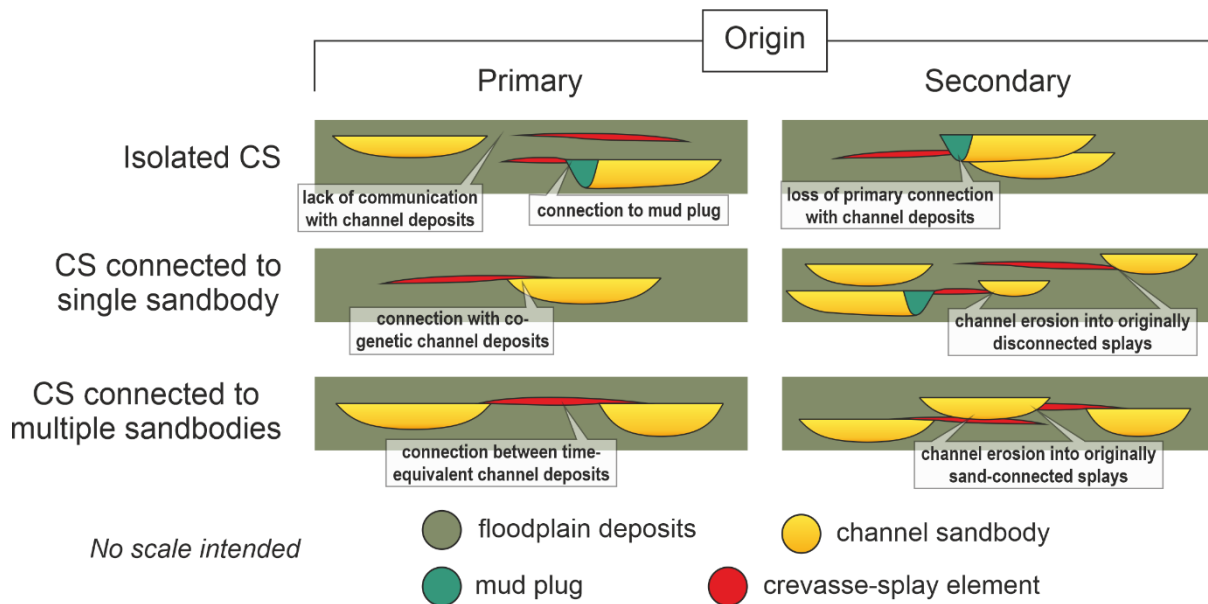


Figure 14: Styles of connectivity of crevasse-splay elements in fluvial successions, in relation to sandbody communication or compartmentalization of primary and secondary origin. Connectivity (or lack thereof) of primary origin is established at the time of deposition, whereas secondary connectivity (or loss thereof) results from juxtaposition of channel and splay elements in relation to erosional reworking of overbank deposits by mobile and avulsive channel forms. CS: crevasse-splay element.

Some of the results also contribute to general understanding of possible geological controls on how crevasse-splay deposits may affect static connectivity. The principal findings can be summarized as follows.

- The volumetric partitioning of net-reservoir volumes across channel and crevasse-splay bodies in fluvial successions can be highly variable. However, some generally applicable relationships are noted: as the proportion of channel bodies increases, the fraction of crevasse-splay deposits tends to decrease overall in the stratigraphy, but tends to increase relative to the volume of overbank deposits (Fig. 8). In the studied analogues, these observations may reflect the following: (i) the close relationship between channels and splays (i.e., increase in the abundance of crevasse splays with the number of channel threads and in parallel with the frequency of avulsion); and (ii) the effect of the erosional reworking of splay bodies by migrating and avulsing channels. Outputs of process-based modelling with FLUMY supports this view (Fig. 11D).
- Based on results of FLUMY simulations, it appears that the formation of isolated crevasse-splay compartments in successions of meandering river systems containing mud-prone abandoned channel fills may be more important – in relative terms – where the width-to-thickness aspect ratios of channel bodies are larger and the net-to-gross ratios is smaller (Fig. 13). This may be because the development of secondary connectivity by lateral channel erosion is less likely under these conditions.
- Overall, positive scaling relationships emerge in the studied analogues (i) between morphometric parameters (thickness, width and length) of crevasse-splay elements, (ii) between the size of crevasse-splay elements and that of channel bodies, channel fills and barforms, and (iii) between the size of crevasse-splay elements and the area of their river catchments (Figs. 5-7). Scaling between the size of river systems and the scale of crevasse splays can be interpreted to reflect controls by the magnitude of formative floods and by along-channel water-surface gradients, which tend to increase and decrease, respectively, with the size of the river systems (Milliman & Farnsworth 2011; Frasson et al. 2019). Nonetheless, the variability in the data is significant, and other factors, which have not been assessed (e.g., accommodation; Millard et al. 2017), may be more important as controls on splay geometry.

- Based on results of object-based stochastic modelling, and assuming the degree of scaling between crevasse-splay and channel sedimentary units seen in the analogues to be typical, the following observations are made: (i) the role of crevasse-splay deposits as connectors of channel bodies is more important for smaller fluvial systems and for lower net-to-gross ratios; (ii) the presence of crevasse-splay deposits as net porous volumes in a succession results in sandbody architectures that may be as broadly connected as purely channelized architectures containing larger net volumes (Fig. 13).

It is significant that the way in which the net-to-gross ratios determines the role of crevasse-splay elements in controlling static connectivity can differ markedly depending on the architecture of the channel sandbodies (i.e., whether they form tanks of sand that are broadly connected internally as opposed to mosaics of barform-scale compartments). In particular, both the influence of splays as connectors between different channel bodies and their likelihood of being compartmentalized by mud plugs may be more important for fluvial systems that are relatively more sand-poor (Figs. 11, 13). Hence, these findings highlight the importance of understanding the likely architectural style of a subsurface succession if predictions of static connectivity based on sand fraction and sandbody geometry are to be attempted.

The results of this work can be applied in contexts of subsurface characterization in the following ways:

- by allowing estimates of the likely contribution of crevasse-splay elements on sandbody connectivity given knowledge of architectural style (channel bodies acting as tanks of sand vs barform-scale compartmentalization), total net-to-gross ratio, and fraction of splay deposits;
- by enabling prediction of the size of crevasse-splay elements where these form isolated compartments, allowing estimations of their likely net volumes and of the likelihood of well intersection;
- by providing constraints with which to ensure that realistic scaling between channel and overbank reservoir units is incorporated in reservoir models and well correlations.

Nevertheless, all insight derived from this work is subject to the limitations in the analogue dataset (mainly relating to data quality, quantity and representativeness; see section 3.1) and in how it is applied. Notably, the influence of the internal lithological organization of crevasse-splay deposits on sandbody connectivity has not been considered. Furthermore, the role of crevasse-splay deposits in controlling the dynamic connectivity of fluvial successions – in relation to their petrophysical heterogeneity and geometric configuration – has not been investigated. This is a topic that deserves further investigation, especially in consideration of the commonly limited permeability of crevasse-splay deposits (Edington & Poeter 2006; Henares et al. 2014; Crooijmans et al. 2016; Willems et al. 2017). Moreover, the process-based modelling work presented in this study was conducted following an approach that was focussed on the reproduction of specified architectural products, according to which the inputs were tuned automatically by FLUMY. To investigate the influence of specific controlling factors on crevasse-splay development and characteristics, a similar analysis could be performed on the results of model runs constrained by variables representing geological boundary conditions (e.g., avulsion frequency, rate of creation of accommodation). Additionally, the ability of object-based modelling algorithm to reproduce the breadth of architectural styles seen in nature is somewhat limited (cf. Colombera et al. 2019), meaning that the related findings of this work should be applied with care. Future work could focus on addressing some of these problems and research topics.

7. Conclusions

The influence of crevasse-splay elements on the static connectivity of subsurface fluvial successions varies depending on the proportion, geometry and topology of its constitutive architectural elements. The importance of these factors has been quantified by integrating information from modern and ancient geological analogues with outputs from stochastic modelling. The results of the analyses are used to summarize how the connectivity of crevasse-splay elements can be categorized in conceptual models of the subsurface. Some of the quantifications find application in workflows of subsurface characterization by providing constraints of geological realism to stochastic and deterministic models. Part of the analysis also elucidates how certain geological factors (e.g., avulsion frequency, conditions

dictating river-system scale) control the static connectivity of fluvial successions containing crevasse-splay sandstones.

Acknowledgements

We thank AkerBP, Areva (now Orano), BHPBilliton, Cairn India (Vedanta), Chevron, CNOOC International, ConocoPhillips, Equinor, Murphy Oil, Occidental, Saudi Aramco, Shell, Tullow Oil, Woodside and YPF for their financial support of the Fluvial, Eolian & Shallow-Marine Research Group at the University of Leeds. We also thank our project partner Petrotechnical Data Systems for their support. LC has been supported by NERC (Catalyst Fund award NE/M007324/1; Follow-on Fund NE/N017218/1). Cathey Burns and Michelle Shiers are acknowledged for contributing to data collection. Fabien Ors and MINES ParisTech are thanked for providing a free license to FLUMY. Two anonymous reviewers are thanked for their constructive comments, which have improved the article.

References

- Aalto, R., Maurice-Bourgoin, L., Dunne, T., Montgomery, D. R., Nittrouer, C. A., & Guyot, J. L. (2003). Episodic sediment accumulation on Amazonian flood plains influenced by El Nino/Southern Oscillation. *Nature*, 425, 493-497.
- Adams, P. N., Slingerland, R. L., & Smith, N. D. (2004). Variations in natural levee morphology in anastomosed channel flood plain complexes. *Geomorphology*, 61, 127-142.
- Allen, J. R. L. (1978). Studies in fluvial sedimentation: an exploratory quantitative model for the architecture of avulsion-controlled alluvial suites. *Sedimentary Geology*, 21, 129-147.
- Ambrose, W. A., & Jackson, M. L. W. (1989). Geologically based infill potential of fluvial gas reservoirs, La Gloria (Frio) Field, South Texas. *South Texas Geological Society Bulletin*, 29, 13-21.
- Ambrose, W. A., Tyler, N., & Parsley, M. J. (1991). Facies heterogeneity, pay continuity, and infill potential in barrier-island, fluvial, and submarine-fan reservoirs: Examples from the Texas Gulf Coast and Midland Basin. In: Miall, A. D., & Tyler, N. (Eds.) *The three-dimensional architecture of terrigenous clastic sediments and its implications for hydrocarbon discovery and recovery*. *SEPM Concepts in Sedimentology and Paleontology*, 3, 13-21.
- Ambrose, W. A., Lakshminarasimhan, S., Holtz, M. H., Núñez-López, V., Hovorka, S. D., & Duncan, I. (2008). Geologic factors controlling CO₂ storage capacity and permanence: case studies based on experience with heterogeneity in oil and gas reservoirs applied to CO₂ storage. *Environmental Geology*, 54, 1619.
- Amorosi, A., Pavesi, M., Lucchi, M. R., Sarti, G., & Piccin, A. (2008). Climatic signature of cyclic fluvial architecture from the Quaternary of the central Po Plain, Italy. *Sedimentary Geology*, 209, 58-68.
- Anderson, D. S. (2005). Architecture of crevasse splay and point-bar bodies of the nonmarine Iles Formation north of Rangely, Colorado: implications for reservoir description. *The Mountain Geologist*, 42, 109-122.
- Arnaud-Fassetta, G. (2013). Dyke breaching and crevasse-splay sedimentary sequences of the Rhône Delta, France, caused by extreme river-flood of December 2003. *Geografia Fisica e Dinamica Quaternaria*, 36, 7-26.
- Arndorfer, D. J. (1973). Discharge patterns in two crevasses of the Mississippi River delta. *Marine Geology*, 15, 269-287.
- Azevêdo, T. M., Nunes, E., & Ramos, C. (2004). Some morphological aspects and hydrological characterization of the Tagus floods in the Santarém region, Portugal. *Natural Hazards*, 31, 587-601.
- Ba, N. T., Quang, T. P. H., Bao, M. L., & Thang, L. P. (2019). Applying multi-point statistical methods to build the facies model for Oligocene formation, X oil field, Cuu Long basin. *Journal of Petroleum Exploration and Production Technology*, 9, 1633-1650.
- Bernal, C., Christophoul, F., Darrozes, J., Laraque, A., Bourrel, L., Soula, J.-C., Guyot, J.-L., & Baby, P. (2013). Crevassing and capture by floodplain drains as a cause of partial avulsion and anastomosis (lower Rio Pastaza, Peru). *Journal of South American Earth Sciences*, 44, 63-74.
- Bersezio, R., Pavia, F., Baio, M., Bini, A., Felletti, F., & Rodondi, C. (2004). Aquifer architecture of the Quaternary alluvial succession of the southern Lambro basin (Lombardy-Italy). *Il Quaternario*, 17, 361-378.

- Bigi, D., Lugli, S., & Fontana, D. (2015). Caratteristiche sedimentologiche dei depositi di ventaglio di rotta prodotti dal Fiume Secchia durante l'alluvione del 19 gennaio 2014 [Sedimentological characteristics of the crevasse-splay deposits of the River Secchia flood of 19th January 2014]. *Atti della Società dei Naturalisti e Matematici di Modena*, 146, 63-69. In Italian with English abstract.
- Bos, I. J., & Stouthamer, E. (2011). Spatial and temporal distribution of sand-containing basin fills in the Holocene Rhine-Meuse delta, the Netherlands. *The Journal of Geology*, 119, 641-660.
- Boucher, A., Gupta, R., Caers, J., & Satija, A. (2010). Tetris: a training image generator for SGeMS. Stanford Center for Reservoir Forecasting.
- Bridge, J. S. (2006). Fluvial facies models: recent developments. In: Posamentier, H. W., & Walker, R. G. (Eds.) *Facies Models Revisited*. SEPM Special Publication 84, 85-170.
- Bridge, J. S., & Leeder, M. R. (1979). A simulation model of alluvial stratigraphy. *Sedimentology*, 26, 617-644.
- Bristow, C., Skelly, R. L., & Ethridge, F. G. (1999). Crevasse splays from the rapidly aggrading, sand bed, braided Niobrara River, Nebraska: effect of base level rise. *Sedimentology*, 46, 1029-1047.
- Bryant, M., Falk, P., & Paola, C. (1995). Experimental study of avulsion frequency and rate of deposition. *Geology*, 23, 365-368.
- Bubnova, A. (2018). Sur le conditionnement des modèles génétiques de réservoirs chenalisés méandriformes à des données de puits – On the conditioning of process-based channelized meandering reservoir models on well data. PhD Thesis, École Nationale Supérieure des Mines de Paris.
- Burns, C. E., Mountney, N. P., Hodgson, D. M., & Colombera, L. (2017). Anatomy and dimensions of fluvial crevasse-splay deposits: Examples from the Cretaceous Castlegate Sandstone and Neslen Formation, Utah, USA. *Sedimentary Geology*, 351, 21-35.
- Burns, C. E., Mountney, N. P., Hodgson, D. M., & Colombera, L. (2019). Stratigraphic architecture and hierarchy of fluvial overbank splay deposits. *Journal of the Geological Society*, 176, 629-649.
- Burns, E. R., Bentley, L. R., Hayashi, M., Grasby, S. E., Hamblin, A. P., Smith, D. G., & Wozniak, P. R. (2010a). Hydrogeological implications of paleo-fluvial architecture for the Paskapoo Formation, SW Alberta, Canada: a stochastic analysis. *Hydrogeology Journal*, 18, 1375-1390.
- Burns, E. R., Bentley, L. R., Therrien, R., & Deutsch, C. V. (2010b). Upscaling facies models to preserve connectivity of designated facies. *Hydrogeology Journal*, 18, 1357-1373.
- Cain, S. (2009). Sedimentology and stratigraphy of a terminal fluvial fan system: the Permian Organ Rock Formation, South East Utah. PhD Thesis, Keele University.
- Cain, S. A., & Mountney, N. P. (2009). Spatial and temporal evolution of a terminal fluvial fan system: the Permian Organ Rock Formation, South-east Utah, USA. *Sedimentology*, 56, 1774-1800.
- Catuneanu, O., & Bowker, D. (2001). Sequence stratigraphy of the Koonap and Middleton fluvial formations in the Karoo foredeep South Africa. *Journal of African Earth Sciences*, 33, 579-595.
- Catuneanu, O., & Elango, H. N. (2001). Tectonic control on fluvial styles: the Balfour Formation of the Karoo Basin, South Africa. *Sedimentary Geology*, 140, 291-313.
- Chapin, M. A., & Mayer, D. F. (1991). Constructing a three-dimensional rock-property model of fluvial sandstones in the Peoria field, Colorado. In: Miall, A. D., & Tyler, N. (Eds.) *The three-dimensional architecture of terrigenous clastic sediments and its implications for hydrocarbon discovery and recovery*. SEPM Concepts in Sedimentology and Paleontology, 3, 160-171.
- Chomiak, L. (2020). Crevasse splays within a lignite seam at the Tomisławice opencast mine near Konin, central Poland: architecture, sedimentology and depositional model. *Geologos*, 26, 25-37.
- Chomiak, L., Maciaszek, P., Wachocki, R., Widera, M., & Zieliński, T. (2019). Seismically-induced soft-sediment deformation in crevasse-splay microdelta deposits (Middle Miocene, central Poland). *Geological Quarterly*, 63, 162-177.
- Cojan, I., Fouche, O., & Lopez, S. (2004). Process-based reservoir modelling in the example meandering channel. In: Leuangthong, O. & Deutsch, C. (Eds.) *Geostatistics Banff 2004*, 611-619. Springer, Dordrecht.

- Colombera, L., Felletti, F., Mountney, N. P., & McCaffrey, W. D. (2012a). A database approach for constraining stochastic simulations of the sedimentary heterogeneity of fluvial reservoirs. *AAPG Bulletin*, 96, 2143-2166.
- Colombera, L., Mountney, N. P., & McCaffrey, W. D. (2012b). A relational database for the digitization of fluvial architecture concepts and example applications. *Petroleum Geoscience*, 18, 129-140.
- Colombera, L., Mountney, N. P., & McCaffrey, W. D. (2013). A quantitative approach to fluvial facies models: Methods and example results. *Sedimentology*, 60, 1526-1558.
- Colombera, L., Shiers, M. N., & Mountney, N. P. (2016). Assessment of backwater controls on the architecture of distributary-channel fills in a tide-influenced coastal-plain succession: Campanian Neslen Formation, USA. *Journal of Sedimentary Research*, 86, 476-497.
- Colombera, L., Mountney, N. P., Russell, C. E., Shiers, M. N., & McCaffrey, W. D. (2017). Geometry and compartmentalization of fluvial meander-belt reservoirs at the bar-form scale: Quantitative insight from outcrop, modern and subsurface analogues. *Marine and Petroleum Geology*, 82, 35-55.
- Colombera, L., Mountney, N. P., Medici, G., & West, L. J. (2019). The geometry of fluvial channel bodies: Empirical characterization and implications for object-based models of the subsurface. *AAPG Bulletin*, 103, 905-929.
- Crooijmans, R. A., Willems, C. J. L., Nick, H. M., & Bruhn, D. F. (2016). The influence of facies heterogeneity on the doublet performance in low-enthalpy geothermal sedimentary reservoirs. *Geothermics*, 64, 209-219.
- Cuevas Gozalo, M. C., & Martinius, A. W. (1993). Outcrop data-base for the geological characterization of fluvial reservoirs: an example from distal fluvial fan deposits in the Loranca Basin, Spain. In: North, C. P., & Prosser, D. J. (Eds.) *Characterization of fluvial and aeolian reservoirs*. Geological Society, London, Special Publication 73, 79-94.
- Dall'Alba, V., Renard, P., Straubhaar, J., Issautier, B., Duvail, C., & Caballero, Y. (2020). 3D multiple-point statistics simulations of the Roussillon Continental Pliocene aquifer using DeeSse. *Hydrology and Earth System Sciences*, 24, 4997-5013.
- Deutsch, C. V., & Tran, T. T. (2002). FLUVSIM: a program for object-based stochastic modeling of fluvial depositional systems. *Computers & Geosciences*, 28, 525-535.
- Donoso, J. M. (2016). *A Contribution to Improve Facies Object Modeling of Meandering Rivers Depositional Systems*. MSc Thesis, Stanford University.
- Donselaar, M. E., & Overeem, I. (2008). Connectivity of fluvial point-bar deposits: An example from the Miocene Huesca fluvial fan, Ebro Basin, Spain. *AAPG Bulletin*, 92, 1109-1129.
- Donselaar, M. E., Gozalo, M. C., & Moyano, S. (2013). Avulsion processes at the terminus of low-gradient semi-arid fluvial systems: lessons from the Río Colorado, Altiplano endorheic basin, Bolivia. *Sedimentary Geology*, 283, 1-14.
- Edgington, D. H. (2003). *Three-dimensional nonlinear-dynamical model of stratal architecture and facies distribution in fluvial environments and its application to problems of fluid flow and transport*. PhD Thesis, Colorado School of Mines, Golden, USA.
- Edgington, D., & Poeter, E. (2006). Stratigraphic control of flow and transport characteristics. *Groundwater*, 44, 826-831.
- Elliott, T. (1974). Interdistributary bay sequences and their genesis. *Sedimentology*, 21, 611-622.
- El-Mowafy, H. Z., & Marfurt, K. J. (2016). Quantitative seismic geomorphology of the middle Frio fluvial systems, south Texas, United States. *AAPG Bulletin*, 100, 537-564.
- Esposito, C. R., Shen, Z., Törnqvist, T. E., Marshak, J., & White, C. (2017). Efficient retention of mud drives land building on the Mississippi Delta plain. *Earth Surface Dynamics*, 5, 387-397.
- Farrell, K. M. (1987). Sedimentology and facies architecture of overbank deposits of the Mississippi River, False River region, Louisiana. In: Ethridge, F. G., Flores, R. M., & Harvey, M. D. (Eds.) *Recent developments in fluvial sedimentology*, SEPM Special Publication 39, 111-120.

- Farrell, K. M. (2001). Geomorphology, facies architecture, and high-resolution, non-marine sequence stratigraphy in avulsion deposits, Cumberland Marshes, Saskatchewan. *Sedimentary Geology*, 139, 93-150.
- Ferguson, R. J., & Brierley, G. J. (1999). Levee morphology and sedimentology along the lower Tuross River, south-eastern Australia. *Sedimentology*, 46, 627-648.
- Fielding, C. R. (1984a). A coal depositional model for the Durham Coal Measures of NE England. *Journal of the Geological Society*, 141, 919-931.
- Fielding, C.R. (1984b). Upper delta plain lacustrine and fluviolacustrine facies from the Westphalian of the Durham coalfield, NE England. *Sedimentology*, 31, 547-567
- Fielding, C.R. (1986). Fluvial channel and overbank deposits from the Westphalian of the Durham coalfield, NE England. *Sedimentology*, 33, 119-140.
- Flores, R. M., & Stricker, G. D. (1993). Early Cenozoic depositional systems, Wishbone Hill District, Matanuska Coal Field, Alaska. *Geologic Studies in Alaska by the US Geological Survey. USGS Bulletin*, 2068, 101-117.
- Florsheim, J. L., & Mount, J. F. (2002). Restoration of floodplain topography by sand-splay complex formation in response to intentional levee breaches, Lower Cosumnes River, California. *Geomorphology*, 44, 67-94.
- Florsheim, J. L., & Mount, J. F. (2003). Changes in lowland floodplain sedimentation processes: pre-disturbance to post-rehabilitation, Cosumnes River, CA. *Geomorphology*, 56, 305-323.
- Ford, G. L., & Pyles, D. R. (2014). A hierarchical approach for evaluating fluvial systems: Architectural analysis and sequential evolution of the high net-sand content, middle Wasatch Formation, Uinta Basin, Utah. *AAPG Bulletin*, 98, 1273-1304.
- Frasson, R. P. d. M., Pavelsky, T. M., Fonstad, M. A., Durand, M. T., Allen, G. H., Schumann, G., Lion, C., Beighley, R. E., & Yang, X. (2019). Global relationships between river width, slope, catchment area, meander wavelength, sinuosity, and discharge. *Geophysical Research Letters*, 46, 3252-3262.
- Galloway, W. E. (1977). Catahoula Formation of the Texas Coastal Plain: depositional systems, composition, structural development, ground-water flow history, and uranium distribution. University of Texas at Austin, Bureau of Economic Geology, Report of Investigations 87.
- Garzón Heydt, G., & Alonso, A. (1996). El río Guadarrama, morfología y sedimentación actual en un cauce arenoso tipo braided. *Cuadernos de Geología Ibérica*, 21, 369-393. In Spanish with English abstract.
- Garzón, G., & Alonso, A. (2002). Comparison of the flood response of a braided and a meandering river, conditioned by anthropogenic and climatic changes. In: Martini, I. P., Baker, V. R., & Garzón G. (Eds.) *Flood and megaflood processes and deposits: Recent and ancient examples*. International Association of Sedimentologists Special Publication 32, 233-249.
- Gębica, P., & Sokołowski, T. (2001). Sedimentological interpretation of crevasse splays formed during the extreme 1997 flood in the upper Vistula River Valley (south Poland). *Annales Societatis Geologorum Poloniae*, 71, 53-62.
- Gębica, P., & Sokołowski, T. (2002). Crevassing of an inland dune during the 1998 flood in upper Vistula river valley (South Poland). *Annales Societatis Geologorum Poloniae*, 72, 191-197.
- Gharibreza, M., Habibi, A., Imamjomeh, S. R., & Ashraf, M. A. (2014). Coastal processes and sedimentary facies in the Zohreh River Delta (northern Persian Gulf). *Catena*, 122, 150-158.
- Ghazi, S., & Mountney, N. P. (2009). Facies and architectural element analysis of a meandering fluvial succession: The Permian Warchha Sandstone, Salt Range, Pakistan. *Sedimentary Geology*, 221, 99-126.
- Gomez, B., Mertes, L. A., Phillips, J. D., Magilligan, F. J., & James, L. A. (1995). Sediment characteristics of an extreme flood: 1993 upper Mississippi River valley. *Geology*, 23, 963-966.
- Gomez, B., Phillips, J. D., Magilligan, F. J., & James, L. A. (1997). Floodplain sedimentation and sensitivity: summer 1993 flood, Upper Mississippi River Valley. *Earth Surface Processes and Landforms*, 22, 923-936.
- Grappe, B. (2014). Modèles d'écoulement à surface libre pour la simulation à long terme de la migration des systèmes méandriformes. PhD Thesis, École Nationale Supérieure des Mines de Paris. In French with English abstract.

- Grappe, B., Cojan, I., Ors, F., & Rivoirard, J. (2016). Dynamic Modelling of Meandering Fluvial Systems at the Reservoir Scale, FLUMY Software. Proceedings of the Second Conference on Forward Modelling of Sedimentary Systems, cp-483-00016. European Association of Geoscientists & Engineers.
- Grasby, S. E., Chen, Z., Hamblin, A. P., Wozniak, P. R., & Sweet, A. R. (2008). Regional characterization of the Paskapoo bedrock aquifer system, southern Alberta. *Canadian Journal of Earth Sciences*, 45, 1501-1516.
- Guion, P. D. (1984). Crevasse splay deposits and roof-rock quality in the Threequarters Seam (Carboniferous) in the East Midlands Coalfield, UK. In: Rahmani, R. A., & Flores, R. M. (Eds.) *Sedimentology of coal and coal-bearing sequences*. International Association of Sedimentologists Special Publication 7, 291-308.
- Guion, P. D., Fulton, I. M., & Jones, N. S. (1995). Sedimentary facies of the coal-bearing Westphalian A and B north of the Wales-Brabant High. Geological Society, London, Special Publication 82, 45-78.
- Gulliford, A. R., Flint, S. S., & Hodgson, D. M. (2017). Crevasse splay processes and deposits in an ancient distributive fluvial system: The lower Beaufort Group, South Africa. *Sedimentary Geology*, 358, 1-18.
- Hajek, E. A., & Edmonds, D. A. (2014). Is river avulsion style controlled by floodplain morphodynamics?. *Geology*, 42, 199-202.
- Hansen, O., Gilding, D., Nazarian, B., Osdal, B., Ringrose, P., Kristoffersen, J.-B., Eiken, O., & Hansen, H. (2013). Snøhvit: The history of injecting and storing 1 Mt CO₂ in the fluvial Tubåen Fm. *Energy Procedia*, 37, 3565-3573.
- Hardage, B. A., Levey, R. A., Pendleton, V., Simmons, J., & Edson, R. (1996). 3-D seismic imaging and interpretation of fluvially deposited thin-bed reservoirs. In: Weimer, P. & Davis, T. L. (Eds.) *Applications of 3-D Seismic Data to Exploration and Production, AAPG Studies in Geology 42 and SEG Geophysical Developments Series 5*, 27-34.
- Hatløy, A. S. (1994). Numerical facies modeling combining deterministic and stochastic methods. In: Yarus, J. M., & Chambers, R. L. (Eds.) *Stochastic modeling and geostatistics. AAPG Computer Applications in Geology 3*, 109-120.
- Heldreich, G., Redfern, J., Legler, B., Gerdes, K., & Williams, B. P. J. (2017). Challenges in characterizing subsurface paralic reservoir geometries: a detailed case study of the Mungaroo Formation, North West Shelf, Australia. In: Hampson, G. J., Reynolds, A. D., Kostic, B., & Wells, M. R. (Eds.) *Sedimentology of Paralic Reservoirs: Recent Advances*. Geological Society, London, Special Publication 444, 59-108.
- Henares, S., Caracciolo, L., Cultrone, G., Fernández, J., & Viseras, C. (2014). The role of diagenesis and depositional facies on pore system evolution in a Triassic outcrop analogue (SE Spain). *Marine and Petroleum Geology*, 51, 136-151.
- Heyvaert, V. M. A., & Walstra, J. (2016). The role of long-term human impact on avulsion and fan development. *Earth Surface Processes and Landforms*, 41, 2137-2152.
- Heyvaert, V. M., Walstra, J., Verkinderen, P., Weerts, H. J., & Ooghe, B. (2012). The role of human interference on the channel shifting of the Karkheh River in the Lower Khuzestan plain (Mesopotamia, SW Iran). *Quaternary International*, 251, 52-63.
- Heyvaert, V. M. A., Walstra, J., & Weerts, H. J. T. (2013). Human impact on avulsion and fan development in a semi-arid region: examples from SW Iran. Proceedings of the 10th International Conference on Fluvial Sedimentology, 14-19 July 2013, Leeds, UK.
- Holzförster, F., Stollhofen, H., & Stanistreet, I. G. (1999). Lithostratigraphy and depositional environments in the Waterberg-Erongo area, central Namibia, and correlation with the main Karoo Basin, South Africa. *Journal of African Earth Sciences*, 29, 105-123.
- Hornung, J., & Aigner, T. (1999). Reservoir and aquifer characterization of fluvial architectural elements: Stubensandstein, Upper Triassic, southwest Germany. *Sedimentary Geology*, 129, 215-280.
- Hovadik, J. M., & Larue, D. K. (2007). Static characterizations of reservoirs: refining the concepts of connectivity and continuity. *Petroleum Geoscience*, 13, 195-211.

- Iacobucci, G., Troiani, F., Milli, S., Mazzanti, P., Piacentini, D., Zocchi, M., & Nadali, D. (2020). Combining Satellite Multispectral Imagery and Topographic Data for the Detection and Mapping of Fluvial Avulsion Processes in Lowland Areas. *Remote Sensing*, 12, 2243.
- Ielpi, A. (2019). Morphodynamics of meandering streams devoid of plant life: Amargosa River, Death Valley, California. *GSA Bulletin*, 131, 782-802.
- Ielpi, A., & Ghinassi, M. (2014). Planform architecture, stratigraphic signature and morphodynamics of an exhumed Jurassic meander plain (Scalby Formation, Yorkshire, UK). *Sedimentology*, 61, 1923-1960.
- Ikeda, S., Parker, G., & Sawai, K. (1981). Bend theory of river meanders. Part 1. Linear development. *Journal of Fluid Mechanics*, 112, 363-377.
- Jacobson, R. B., & Oberg, K. A. (1997). Geomorphic changes on the Mississippi River flood plain at Miller City, Illinois, as a result of the flood of 1993 (Vol. 1120). USGS Circular 1120-J. US Government Printing Office.
- Jirik, L. A. (1990). Reservoir heterogeneity in middle Frio fluvial sandstones: case studies in Seeligson field, Jim Wells County, Texas. *Gulf Coast Association of Geological Societies Transactions*, 40, 335-352.
- Joeckel, R. M., Tucker, S. T., & McMullin, J. D. (2016). Morphosedimentary features from a major flood on a small, lower-sinuosity, single-thread river: The unknown quantity of overbank deposition, historical-change context, and comparisons with a multichannel river. *Sedimentary Geology*, 343, 18-37.
- Jones, H. L., & Hajek, E. A. (2007). Characterizing avulsion stratigraphy in ancient alluvial deposits. *Sedimentary Geology*, 202, 124-137.
- Jones, J. R., Scott, A. J., & Lake, L. W. (1987). The geologic aspects of reservoir characterization for numerical simulation: Mesaverde meanderbelt sandstone, northwestern Colorado. *SPE Formation Evaluation*, 2, 97-107.
- Jordan, D. W., & Pryor, W. A. (1992). Hierarchical levels of heterogeneity in a Mississippi River meander belt and application to reservoir systems. *AAPG Bulletin*, 76, 1601-1624.
- Jorgensen, P. J., & Fielding, C. R. (1996). Facies architecture of alluvial floodbasin deposits: three-dimensional data from the Upper Triassic Callide Coal Measures of east-central Queensland, Australia. *Sedimentology*, 43, 479-495.
- Jotheri, J. (2018). Recognition criteria for canals and rivers in the Mesopotamian floodplain. In: Altaweel, M., & Zhuang, Y. (Eds.) *Water societies and technologies from the past and present*, 109-126. UCL Press, London.
- Jotheri, J., Altaweel, M., Tuji, A., Anma, R., Pennington, B., Rost, S., & Watanabe, C. (2018). Holocene fluvial and anthropogenic processes in the region of Uruk in southern Mesopotamia. *Quaternary International*, 483, 57-69.
- Jotheri J., Allen M. B. (2020) Recognition of ancient channels and archaeological sites in the Mesopotamian floodplain using satellite imagery and digital topography. In: Lawrence, D., Altaweel, M., & Philip, G. (Eds.) *New Agenda in Remote Sensing and Landscape Archaeology in the Near East: Studies in Honor of T.J. Wilkinson*, 283-305. Archaeopress, Oxford.
- Journel, A. G., & Xu, W. (1994). Posterior identification of histograms conditional to local data. *Mathematical Geology*, 26, 323-359.
- Keogh, K. J., Martinius, A. W., & Osland, R. (2007). The development of fluvial stochastic modelling in the Norwegian oil industry: A historical review, subsurface implementation and future directions. *Sedimentary Geology*, 202, 249-268.
- Kesel, R. H. (1988). The decline in the suspended load of the lower Mississippi River and its influence on adjacent wetlands. *Environmental Geology and Water Sciences*, 11, 271-281.
- Kraus, M. J., & Middleton, L. T. (1987). Contrasting Architecture of two Alluvial Suites in Different Structural Settings. In: Ethridge, F. G., Flores, R. M., & Harvey, M. D. (Eds.) *Recent Developments in Fluvial Sedimentology*, SEPM Special Publication 39, 253-262.
- Kurowski, L. (1999). Formy akumulacji piasku na równi zalewowej Odry między Koźlem a ujściem Kłodnicy [Sand accumulation forms on the flood plain of the Odra river between Koźle city and mouth of the Kłodnica river (SW Poland)]. *Przegląd Geologiczny*, 47, 194-198. In Polish with English abstract.

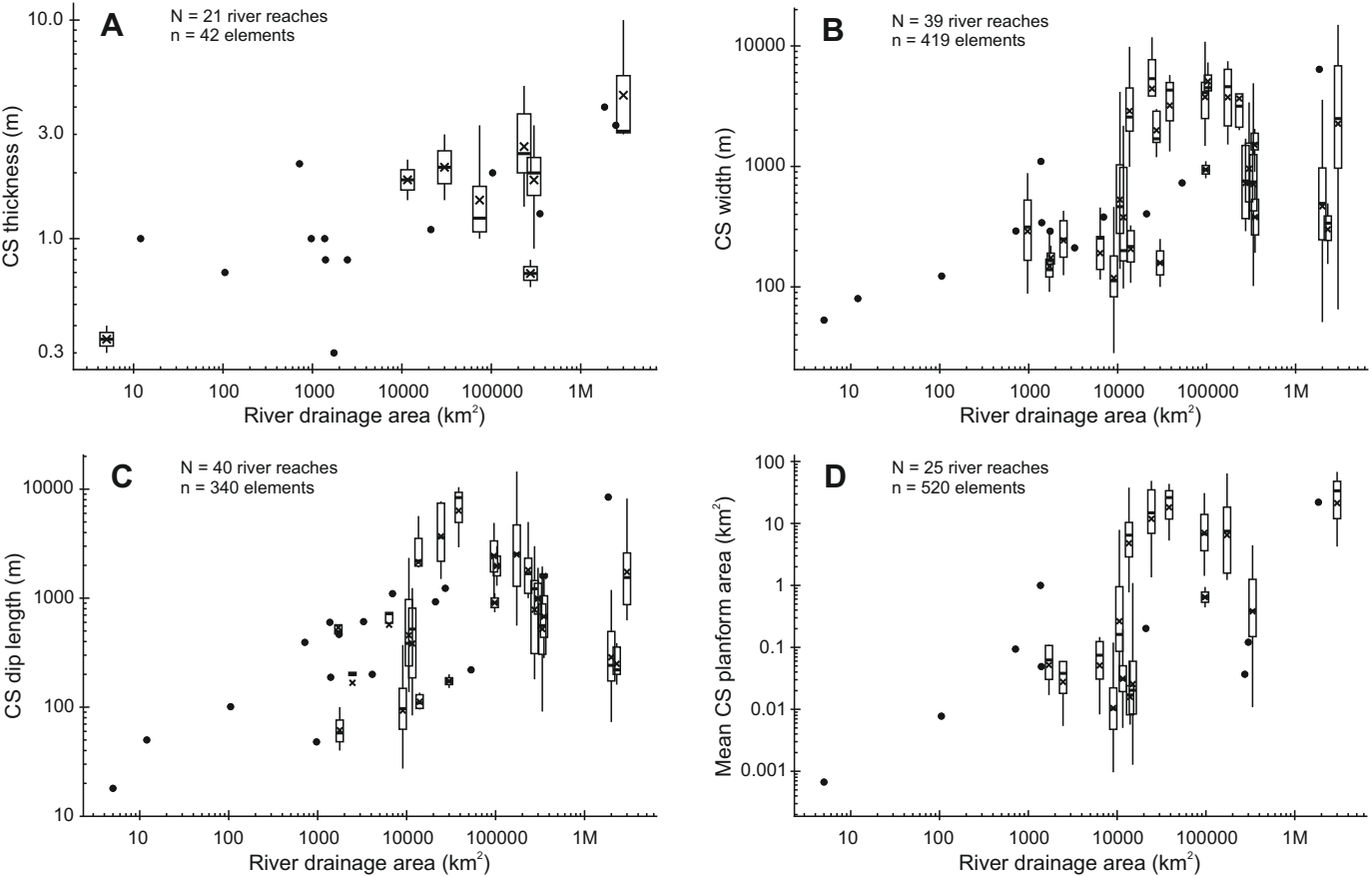
- Labourdette, R. (2011). Stratigraphy and static connectivity of braided fluvial deposits of the lower Escanilla Formation, south central Pyrenees, Spain. *AAPG Bulletin*, 95, 585-617.
- Lamb, M. P., Nittrouer, J. A., Mohrig, D., & Shaw, J. (2012). Backwater and river plume controls on scour upstream of river mouths: Implications for fluvio-deltaic morphodynamics. *Journal of Geophysical Research: Earth Surface*, 117, F01002.
- Lang, S. C., Kassin, J., Benson, J., Grasso, C., Hicks, T., Hall, N., & Avenell, C. (2002). Reservoir characterisation of fluvial, lacustrine and deltaic successions—Applications of modern and ancient geological analogues. *Proceedings of the 28th Annual Convention of the Indonesian Petroleum Association*, 1, 557-580.
- Larue, D. K., & Hovadik, J. (2006). Connectivity of channelized reservoirs: a modelling approach. *Petroleum Geoscience*, 12, 291-308.
- Lew, C. L., Ismail, H. H., Kadir, M. F., & Tajuddin, M. R. (2016). Stratal Slicing: A Tool for Imaging Geologically Time-Equivalent Fluvial Architecture-A Field Case Study. *International Petroleum Technology Conference*, Bangkok, 14-16 November 2016, IPTC-18599-MS.
- Lewin, J., Ashworth, P. J., & Strick, R. J. (2017). Spillage sedimentation on large river floodplains. *Earth Surface Processes and Landforms*, 42, 290-305.
- Li, Jiaguang, Luthi, S. M., Donselaar, M. E., Weltje, G. J., Prins, M. A., & Bloemsma, M. R. (2015). An ephemeral meandering river system: Sediment dispersal processes in the Río Colorado, Southern Altiplano Plateau, Bolivia. *Zeitschrift für Geomorphologie*, 59, 301-317.
- Li, Jun, Zhang, X., Lu, B., Ahmed, R., & Zhang, Q. (2019). Static Geological Modelling with Knowledge Driven Methodology. *Energies*, 12, 3802.
- Limarino, C., Tripaldi, A., Marensi, S., Net, L., Re, G., & Caselli, A. (2001). Tectonic control on the evolution of the fluvial systems of the Vinchina Formation (Miocene), northwestern Argentina. *Journal of South American Earth Sciences*, 14, 751-762.
- Lopez, S. (2003). Modélisation de réservoirs chenalisés méandriiformes: une approche génétique et stochastique. PhD Thesis, École Nationale Supérieure des Mines de Paris. In French.
- Ma, Y. Z., Gomez, E., Luneau, B., Iwere, F., Young, T. J., & Cox, D. L. (2011). Integrated reservoir modeling of a Pinedale tight-gas reservoir in the Greater Green River Basin, Wyoming. In: Ma, Y. Z., & La Pointe, P. R. (Eds.) *Uncertainty analysis and reservoir modeling*. AAPG Memoir 96, 89-106.
- Mack, G. H., Leeder, M., Perez-Arlucea, M., & Bailey, B. D. (2003). Early Permian silt-bed fluvial sedimentation in the Orogrande basin of the Ancestral Rocky Mountains, New Mexico, USA. *Sedimentary Geology*, 160, 159-178.
- Makaske, B. (2001). Anastomosing rivers: a review of their classification, origin and sedimentary products. *Earth-Science Reviews*, 53, 149-196.
- Makaske, B., Smith, D. G., & Berendsen, H. J. (2002). Avulsions, channel evolution and floodplain sedimentation rates of the anastomosing upper Columbia River, British Columbia, Canada. *Sedimentology*, 49, 1049-1071.
- Makaske, B., Lavooi, E., de Haas, T., Kleinhans, M. G., & Smith, D. G. (2017). Upstream control of river anastomosis by sediment overloading, upper Columbia River, British Columbia, Canada. *Sedimentology*, 64, 1488-1510.
- Maliva, R. G. (2016). *Aquifer characterization techniques*. Springer, Berlin.
- Mastrocicco, M., Colombani, N., Palpacelli, S., & Castaldelli, G. (2011). Large tank experiment on nitrate fate and transport: the role of permeability distribution. *Environmental Earth Sciences*, 63, 903-914.
- Matsumoto, D., Sawai, Y., Yamada, M., Namegaya, Y., Shinozaki, T., Takeda, D., Fujino, S., Tanigawa, K., Nakamura, A., & Pilarczyk, J. E. (2016). Erosion and sedimentation during the September 2015 flooding of the Kinu River, central Japan. *Scientific Reports*, 6, 1-10.
- McKenna, S. A., & Smith, G. (2004). Sensitivity of groundwater flow patterns to parameterization of object-based fluvial aquifer models. In: Bridge, J., & Hyndman D. (Eds.) *Aquifer characterization*, SEPM Special Publication 80, 29-41.

- Meybeck, M., Laroche, L., Dürr, H. H., & Syvitski, J. P. M. (2003). Global variability of daily total suspended solids and their fluxes in rivers. *Global and Planetary Change*, 39, 65-93.
- Miall, A. D. (1996). *The geology of fluvial deposits: sedimentary facies, basin analysis, and petroleum geology*. Springer, Berlin.
- Miall, A. D. (2014). *Fluvial depositional systems*. Springer, Berlin.
- Millard, C., Hajek, E., & Edmonds, D. A. (2017). Evaluating controls on crevasse-splay size: implications for floodplain-basin filling. *Journal of Sedimentary Research*, 87, 722-739.
- Milliman, J. D., & Farnsworth, K. L. (2011). *River discharge to the coastal ocean: a global synthesis*. Cambridge University Press.
- Mjøs, R., Walderhaug, O., & Prestholm, E. (1993). Crevasse splay sandstone geometries in the Middle Jurassic Ravenscar Group of Yorkshire, UK. In: Marzo, M., & Puigdefàbregas, C. (Eds.) *Alluvial sedimentation*. International Association of Sedimentologists Special Publication 17, 167-184.
- Mohrig, D., Heller, P. L., Paola, C., & Lyons, W. J. (2000). Interpreting avulsion process from ancient alluvial sequences: Guadalupe-Matarranya system (northern Spain) and Wasatch Formation (western Colorado). *Geological Society of America Bulletin*, 112, 1787-1803.
- Morozova, G. S. (2005). A review of Holocene avulsions of the Tigris and Euphrates rivers and possible effects on the evolution of civilizations in lower Mesopotamia. *Geoarchaeology*, 20, 401-423.
- Nichols, A. L., & Viers, J. H. (2017). Not all breaks are equal: Variable hydrologic and geomorphic responses to intentional levee breaches along the lower Cosumnes River, California. *River Research and Applications*, 33, 1143-1155.
- Nienhuis, J. H. (2019). River delta floodplains: diffusive deposition, crevasse splays, or avulsions? *Proceedings of Land of Rivers: NCR DAYS 2019*, Utrecht University, 104-105.
- Nienhuis, J. H., Törnqvist, T. E., & Esposito, C. R. (2018). Crevasse splays versus avulsions: a recipe for land building with levee breaches. *Geophysical Research Letters*, 45, 4058-4067.
- Nittrouer, J. A., Shaw, J., Lamb, M. P., & Mohrig, D. (2012). Spatial and temporal trends for water-flow velocity and bed-material sediment transport in the lower Mississippi River. *GSA Bulletin*, 124, 400-414.
- Nordahl, K., Messina, C., Berland, H., Rustad, A. B., & Rimstad, E. (2014). Impact of multiscale modelling on predicted porosity and permeability distributions in the fluvial deposits of the Upper Lunde Member (Snorre Field, Norwegian Continental Shelf). In: Martinius, A. W., Howell, J. A., & Good, T. (Eds.) *Sediment-body geometry and heterogeneity: analogue studies for modelling the subsurface*. Geological Society, London, Special Publication 387, 85-109.
- O'Brien, P. E., & Wells, A. T. (1986). A small, alluvial crevasse splay. *Journal of Sedimentary Research*, 56, 876-879.
- Olsen, H. (1989). Sandstone-body structures and ephemeral stream processes in the Dinosaur Canyon Member, Moenave Formation (Lower Jurassic), Utah, USA. *Sedimentary Geology*, 61, 207-221.
- Ori, G. G., & Penney, S. R. (1982). The stratigraphy and sedimentology of the Old Red Sandstone sequence at Dunmore East, County Waterford. *Journal of Earth Sciences*, Royal Dublin Society, 5, 43-59.
- Ortega, J. A., & Garzón Heydt, G. (2009). Geomorphological and sedimentological analysis of flash-flood deposits: The case of the 1997 Rivillas flood (Spain). *Geomorphology*, 112, 1-14.
- Pardo-Igúzquiza, E., & Dowd, P. A. (2003). CONNEX3D: a computer program for connectivity analysis of 3D random set models. *Computers & Geosciences*, 29, 775-785.
- Perdomo Figueroa, C. (2017). *Floodplain aggradation in a semi-arid endorheic basin setting, Altiplano, Bolivia*. MSc Thesis, Delft University of Technology, Delft, The Netherlands.
- Pérez-Arlucea, M., & Smith, N. D. (1999). Depositional patterns following the 1870s avulsion of the Saskatchewan River (Cumberland marshes, Saskatchewan, Canada). *Journal of Sedimentary Research*, 69, 62-73.

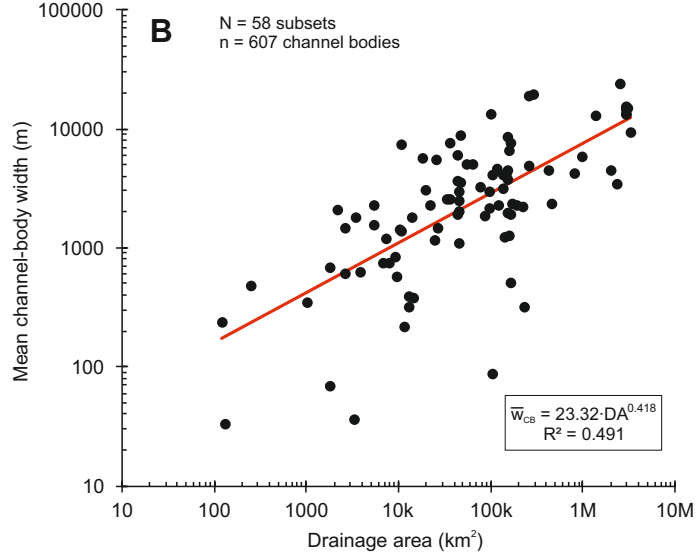
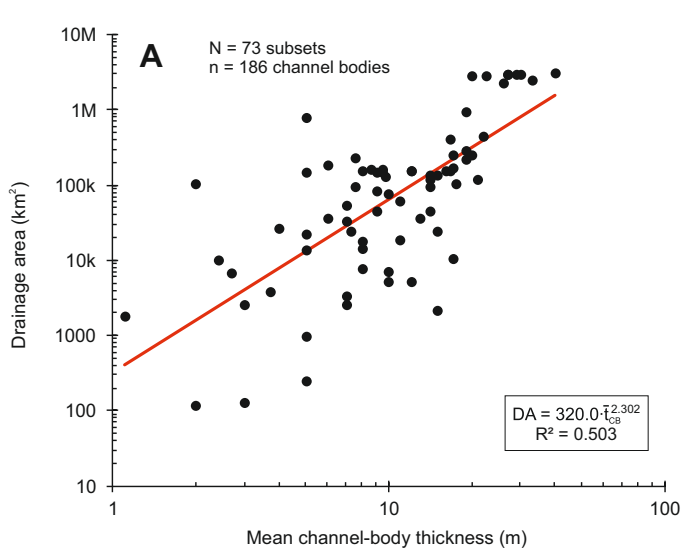
- Pranter, M. J., & Sommer, N. K. (2011). Static connectivity of fluvial sandstones in a lower coastal-plain setting: An example from the Upper Cretaceous lower Williams Fork Formation, Piceance Basin, Colorado. *AAPG Bulletin*, 95, 899-923.
- Pranter, M. J., Cole, R. D., Panjaitan, H., & Sommer, N. K. (2009). Sandstone-body dimensions in a lower coastal-plain depositional setting: lower Williams Fork Formation, Coal Canyon, Piceance Basin, Colorado. *AAPG Bulletin*, 93, 1379-1401.
- Ramón, J. C., & Cross, T. (1997). Characterization and prediction of reservoir architecture and petrophysical properties in fluvial channel sandstones, middle Magdalena Basin, Colombia. *CT&F-Ciencia, Tecnología y Futuro*, 1, 19-46.
- Rasmussen, A. M. S. (2005). Reservoir characterization of a fluvial sandstone: depositional environment and heterogeneities in modeling of the Colton Formation, Utah. MSc Thesis, University of Oslo.
- Reid, I., & Frostick, L. E. (2011). Channel form, flows and sediments of endogenous ephemeral rivers in deserts. In: Thomas T. S. G. (Ed.) *Arid zone geomorphology: Process, form and change in drylands*, third edition, 301-332.
- Remy, N., Boucher, A., & Wu, J. (2009). *Applied geostatistics with SGeMS: a user's guide*. Cambridge University Press.
- Renard, P., & Allard, D. (2013). Connectivity metrics for subsurface flow and transport. *Advances in Water Resources*, 51, 168-196.
- Reynolds, A. D. (1999). Dimensions of paralic sandstone bodies. *AAPG Bulletin*, 83, 211-229.
- Roberts, E. M. (2007). Facies architecture and depositional environments of the Upper Cretaceous Kaiparowits Formation, southern Utah. *Sedimentary Geology*, 197, 207-233.
- Rygel, M. C., & Gibling, M. R. (2006). Natural geomorphic variability recorded in a high-accommodation setting: fluvial architecture of the Pennsylvanian Joggins Formation of Atlantic Canada. *Journal of Sedimentary Research*, 76, 1230-1251.
- Sánchez-Moya, Y., Sopeña, A., & Ramos, A. (1996). Infill architecture of a nonmarine half-graben Triassic basin (central Spain). *Journal of Sedimentary Research*, 66, 1122-1136.
- Sahoo, H., Gani, M. R., Hampson, G. J., Gani, N. D., & Ranson, A. (2016). Facies-to sandbody-scale heterogeneity in a tight-gas fluvial reservoir analog: Blackhawk Formation, Wasatch Plateau, Utah, USA. *Marine and Petroleum Geology*, 78, 48-69.
- Sato, Y., Yoshinori, M., Urabe, A., Komatsubara, J., & Naya, T. (2017). Crevasse splay deposits of the 2015 Kanto-Tohoku Torrential Rain Disaster in the central part of the Kinu River, Kami-Misaka district, Joso City. *The Quaternary Research*, 56, 37-50. In Japanese with English abstract.
- Sendziak, K. L. (2012). Stratigraphic architecture and avulsion deposits of a low net-sand content fluvial succession: Lower Wasatch Formation, Uinta Basin. MSc Thesis, Colorado School of Mines, Golden, USA.
- Shen, Z., Törnqvist, T. E., Mauz, B., Chamberlain, E. L., Nijhuis, A. G., & Sandoval, L. (2015). Episodic overbank deposition as a dominant mechanism of floodplain and delta-plain aggradation. *Geology*, 43, 875-878.
- Shiers, M. N. (2016). Controls on the deposition, accumulation and preservation of mixed fluvial and marginal-marine successions in coastal-plain settings. PhD Thesis, University of Leeds.
- Slingerland, R., & Smith, N. D. (1998). Necessary conditions for a meandering-river avulsion. *Geology*, 26, 435-438.
- Slingerland, R., & Smith, N. D. (2004). River avulsions and their deposits. *Annual Review of Earth and Planetary Sciences*, 32, 257-285.
- Sloan, J. A. (2012). Stratigraphic architecture and connectivity of a low net-to-gross fluvial system: Combining outcrop analogs and multiple-point geostatistical modeling, lower Williams Fork Formation, Piceance Basin, Colorado. MSc Thesis, University of Colorado at Boulder.
- Słowik, M. (2018). The formation of an anabranching planform in a sandy floodplain by increased flows and sediment load. *Earth Surface Processes and Landforms*, 43, 623-638.

- Smith, N. D., & Pérez-Arlucea, M. (1994). Fine-grained splay deposition in the avulsion belt of the lower Saskatchewan River, Canada. *Journal of Sedimentary Research*, 64, 159-168.
- Smith, N. D., Cross, T. A., Dufficy, J. P., & Clough, S. R. (1989). Anatomy of an avulsion. *Sedimentology*, 36, 1-23.
- Smith, R. M. H. (1987). Morphology and depositional history of exhumed Permian point bars in the southwestern Karoo, South Africa. *Journal of Sedimentary Research*, 57, 19-29.
- Staub, J. R., & Cohen, A. D. (1979). The Snuggedy Swamp of South Carolina; a back-barrier estuarine coal-forming environment. *Journal of Sedimentary Research*, 49, 133-143.
- Stewart, D. J. (1983). Possible suspended-load channel deposits from the Wealden Group (Lower Cretaceous) of southern England. In: Collinson, J. D., & Lewin, J. (Eds.) *Modern and ancient fluvial systems*. International Association of Sedimentologists Special Publication 6, 369-384.
- Stuart, J. Y., Mountney, N. P., McCaffrey, W. D., Lang, S. C., & Collinson, J. D. (2014). Prediction of channel connectivity and fluvial style in the flood-basin successions of the Upper Permian Rangal Coal Measures (Queensland). *AAPG Bulletin*, 98, 191-212.
- Syvitski, J. P., Overeem, I., Brakenridge, G. R., & Hannon, M. (2012). Floods, floodplains, delta plains—a satellite imaging approach. *Sedimentary Geology*, 267, 1-14.
- Toonen, W. H., van Asselen, S., Stouthamer, E., & Smith, N. D. (2016). Depositional development of the Muskeg Lake crevasse splay in the Cumberland Marshes (Canada). *Earth Surface Processes and Landforms*, 41, 117-129.
- Trendell, A. M., Atchley, S. C., & Nordt, L. C. (2013). Facies analysis of a probable large-fluvial-fan depositional system: the Upper Triassic Chinle Formation at Petrified Forest National Park, Arizona, USA. *Journal of Sedimentary Research*, 83, 873-895.
- Turner, B. R., & Tester, G. N. (2006). The Table Rocks Sandstone: A fluvial, friction-dominated lobate mouth bar sandbody in the Westphalian B Coal Measures, NE England. *Sedimentary Geology*, 190, 97-119.
- Tye, R. S. (2013). Quantitatively modeling alluvial strata for reservoir development with examples from Krasnoleninskoye field, Russia. *Journal of Coastal Research*, 69, 129-152.
- Van de Lageweg, W. I., van Dijk, W. M., & Kleinmans, M. G. (2013). Morphological and stratigraphical signature of floods in a braided gravel-bed river revealed from flume experiments. *Journal of Sedimentary Research*, 83, 1033-1046.
- Van Dinter, M., & van Zijverden, W. K. (2010). Settlement and land use on crevasse splay deposits; geoarchaeological research in the Rhine-Meuse Delta, the Netherlands. *Netherlands Journal of Geosciences*, 89, 21-34.
- Van Toorenburg, K. A., Donselaar, M. E., Noordijk, N. A., & Weltje, G. J. (2016). On the origin of crevasse-splay amalgamation in the Huesca fluvial fan (Ebro Basin, Spain): Implications for connectivity in low net-to-gross fluvial deposits. *Sedimentary Geology*, 343, 156-164.
- Van Toorenburg, K. A., Donselaar, M. E., & Weltje, G. J. (2018). The life cycle of crevasse splays as a key mechanism in the aggradation of alluvial ridges and river avulsion. *Earth Surface Processes and Landforms*, 43, 2409-2420.
- Vevle, M. L., Aarnes, I., Ledsaak, K., Hauge, R., & Skorstad, A. (2018, June). Facies modelling of a real-life fluvial system using a modern object-based algorithm. *Proceedings of the 80th EAGE Conference and Exhibition 2018*. European Association of Geoscientists & Engineers.
- Visser, J. N. J., & Botha, B. J. V. (1980). Meander channel, point bar, crevasse splay and aeolian deposits from the Elliot Formation in Barkly Pass, north-eastern Cape. *South African Journal of Geology*, 83, 55-62.
- Walstra, J., Heyvaert, V. M. A., & Verkinderen, P. (2010). Assessing human impact on alluvial fan development: a multidisciplinary case-study from Lower Khuzestan (SW Iran). *Geodinamica Acta*, 23, 267-285.
- Webber, K. J., & van Geuns, L. C. (1990). Framework for constructing clastic reservoir simulation models. *Journal of Petroleum Technology*, 42, 1248-1297.

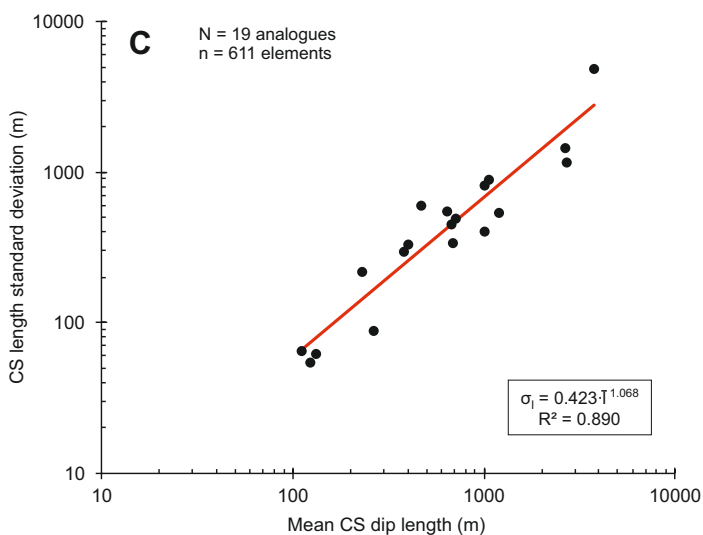
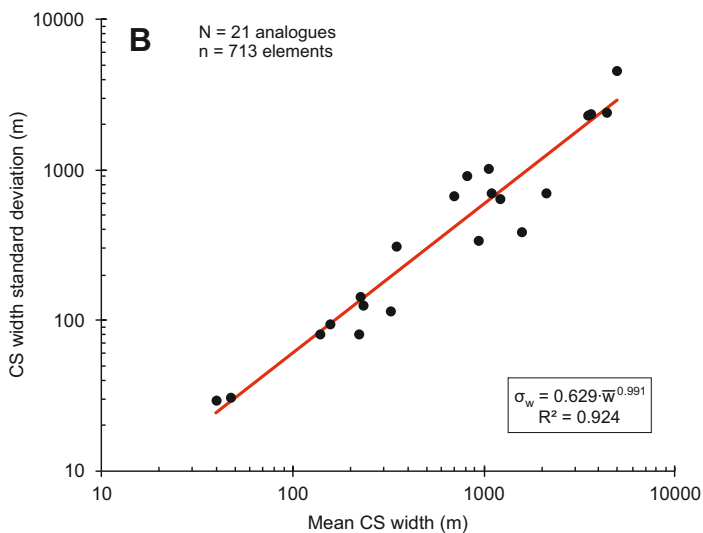
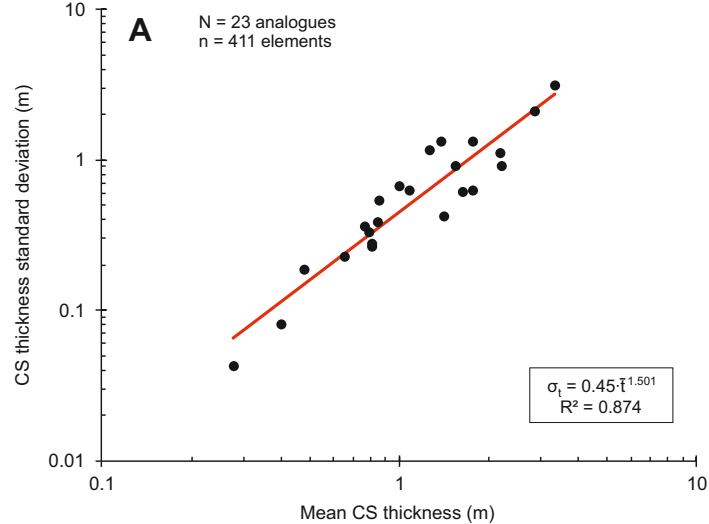
- Weerts, H. J., & Bierkens, M. F. (1993). Geostatistical analysis of overbank deposits of anastomosing and meandering fluvial systems; Rhine-Meuse delta, The Netherlands. In: Fielding C. R. (Ed.) *Current Research in Fluvial Sedimentology*. *Sedimentary Geology*, 85, 221-232.
- Widera, M. (2016). Depositional environments of overbank sedimentation in the lignite-bearing Grey Clays Member: New evidence from Middle Miocene deposits of central Poland. *Sedimentary Geology*, 335, 150-165.
- Wilkinson, T. J., Rayne, L., & Jotheri, J. (2015). Hydraulic landscapes in Mesopotamia: The role of human niche construction. *Water History*, 7, 397-418.
- Willems, C. J., Nick, H. M., Donselaar, M. E., Weltje, G. J., & Bruhn, D. F. (2017). On the connectivity anisotropy in fluvial Hot Sedimentary Aquifers and its influence on geothermal doublet performance. *Geothermics*, 65, 222-233.
- Williams, G. P. (1989). Sediment concentration versus water discharge during single hydrologic events in rivers. *Journal of Hydrology*, 111, 89-106.
- Wright, L. D. (1985). River deltas. In: Davis Jr., R. A. (Ed.) *Coastal sedimentary environments*, 2nd edition, 1-76. Springer, New York.
- Xu, J., Snedden, J. W., Galloway, W. E., Milliken, K. T., & Blum, M. D. (2017). Channel-belt scaling relationship and application to early Miocene source-to-sink systems in the Gulf of Mexico basin. *Geosphere*, 13, 179-200.
- Yan, N., Colombera, L., Mountney, N., & Dorrell, R. M. (2019). Fluvial point-bar architecture and facies heterogeneity, and their influence on intra-bar static connectivity in humid coastal-plain and dryland fan systems. In: Ghinassi, M., Colombera, L., Mountney, N. P., & Reesink, A. J. H. (Eds.) *Fluvial Meanders and Their Sedimentary Products in the Rock Record*. International Association of Sedimentologists Special Publication 48, 475-508.
- Yeste L. M., Varela A. N., Viseras C., McDougall N. D., García-García F. (2020) Reservoir architecture and heterogeneity distribution in floodplain sandstones: Key features in outcrop, core and wireline logs. *Sedimentology*, in press.
- Yu, Y., Shi, X., Wang, H., Yue, C., Chen, S., Liu, Y., Hu, L., & Qiao, S. (2013). Effects of dams on water and sediment delivery to the sea by the Huanghe (Yellow River): The special role of Water-Sediment Modulation. *Anthropocene*, 3, 72-82.
- Yuill, B. T., Khadka, A. K., Pereira, J., Allison, M. A., & Meselhe, E. A. (2016). Morphodynamics of the erosional phase of crevasse-splay evolution and implications for river sediment diversion function. *Geomorphology*, 259, 12-29.
- Zwoliński, Z. (1992). Sedimentology and geomorphology of overbank flows on meandering river floodplains. *Geomorphology*, 4, 367-379.



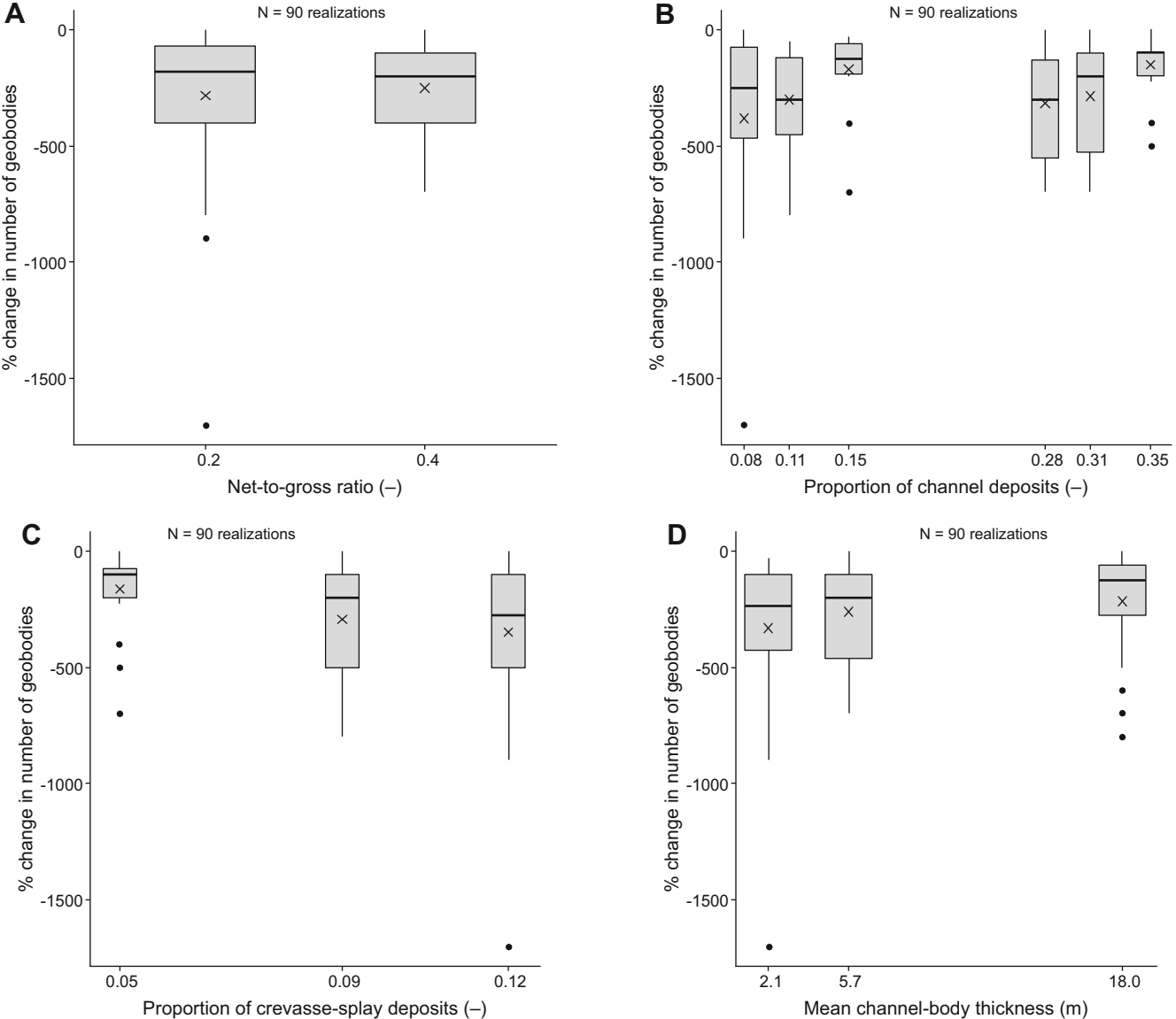
Supplementary Figure 1: Distributions in crevasse-splay thickness (A), cross-floodplain width (B), dip length (C), and planform area (D) for different values of river drainage area. Spots indicate single values of each morphometric parameter. In boxplots, boxes represent interquartile ranges, horizontal bars in boxes represent medians, and crosses (x) represent means.



Supplementary Figure 2: Scaling relationships between river catchment size and channel-body morphometric parameters. (A) Relationship between river drainage area and mean channel-body thickness. (B) Relationship between mean channel-body width and river drainage area.



Supplementary Figure 3: Relationships between mean and standard-deviation values of crevasse-splay morphometric parameters in the studied analogues. Standard deviations are related to corresponding mean values of crevasse-splay thickness (A), width (B), and dip length (C).



Supplementary Figure 4: Distributions in the relative change (expressed in percentage) in the number of geobodies caused by inclusion of crevasse-splay deposits, seen across TETRIS object-based models grouped by: input net-to-gross ratio (A), input proportion of channel (B) and crevasse-splay (C) deposits, and mean channel-body thickness (D). A larger decrease in the number of geobodies (i.e., negative values that are larger in module) denotes a more significant increase in connectivity associated with the inclusion of crevasse-splay elements. Boxes represent interquartile ranges, horizontal bars in boxes represent medians, and crosses (x) represent means.